



Finanziato
dall'Unione europea
NextGenerationEU



Ministero
dell'Università
e della Ricerca



Italiadomani
PIANO NAZIONALE
DI RIPRESA E RESILIENZA



Dipartimento
di Fisica
e Astronomia

UNIVERSITÀ DEGLI STUDI DI PADOVA

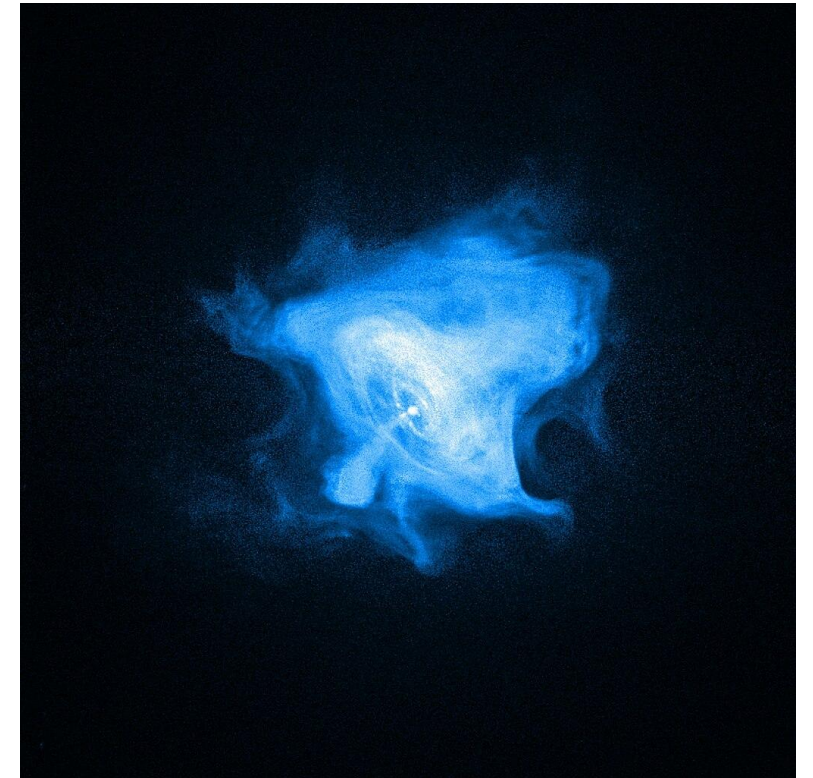
Agenzia Spaziale Italiana Explorer

X-ray polarimetry: Highly magnetized sources

ASI School on IXPE data analysis for general observers
February 19-23, 2024

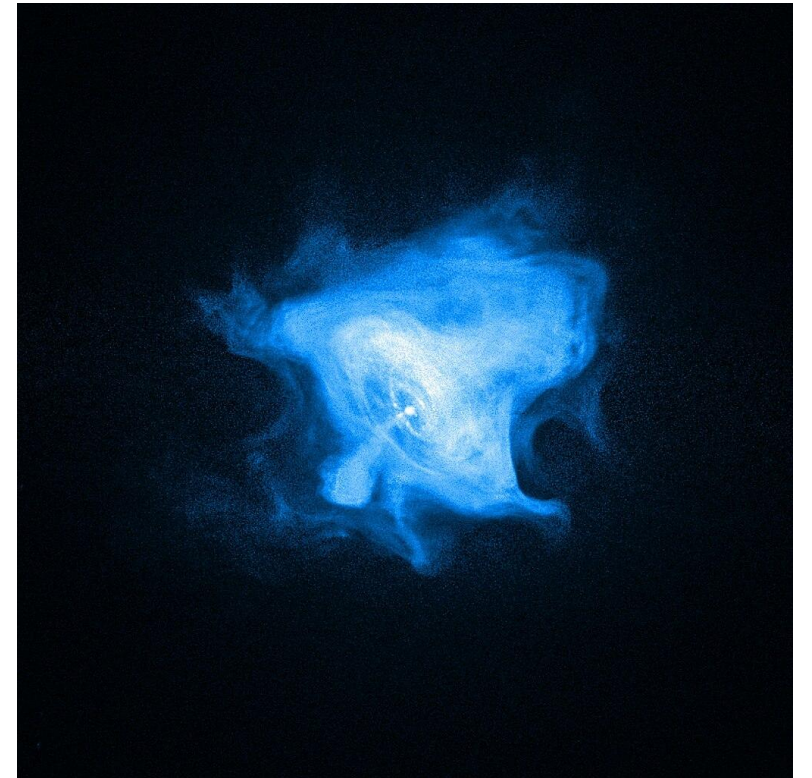
Neutron stars: general notions

- Neutron stars (NSs) are relics of massive stars ($M_{\text{prog}} \approx 8 - 25 M_{\odot}$)
 - Masses $M_{\text{NS}} \approx 1 - 2 M_{\odot}$
 - Radii $R_{\text{NS}} \approx 10 - 15 \text{ km}$
- } $\rho_{\text{m}} \approx 10^{14} - 10^{15} \text{ g/cm}^3$
- Indeed made of neutrons (mostly, typically 8 n every p^+ / e^-) – sustained by the pressure of degenerate neutrons



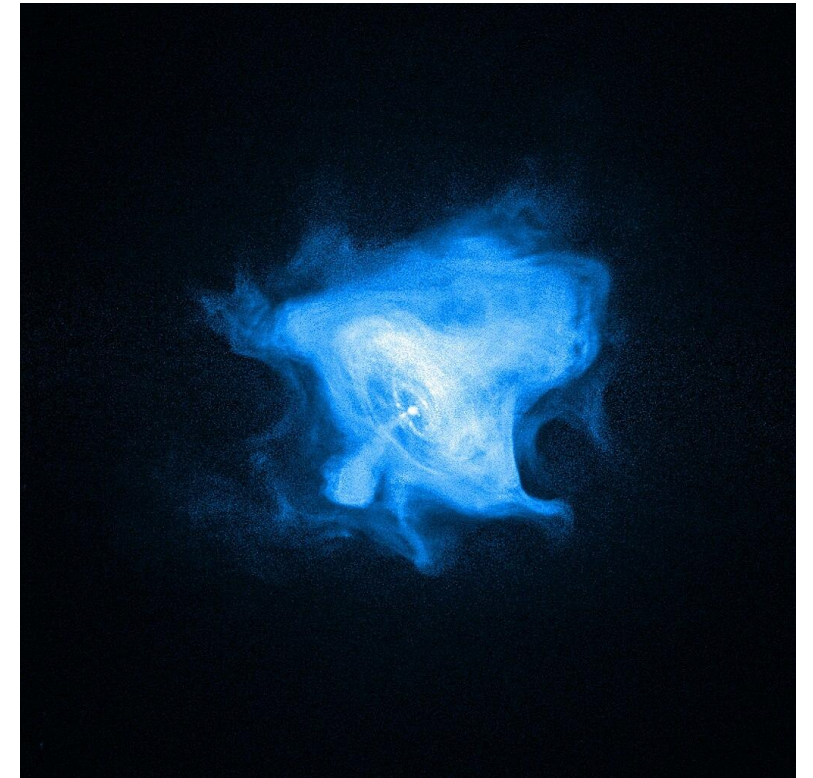
Neutron stars: general notions

- Neutron stars (NSs) are relics of massive stars ($M_{\text{prog}} \approx 8 - 25 M_{\odot}$)
 - Masses $M_{\text{NS}} \approx 1 - 2 M_{\odot}$
 - Radii $R_{\text{NS}} \approx 10 - 15 \text{ km}$
- } $\rho_{\text{m}} \approx 10^{14} - 10^{15} \text{ g/cm}^3$
- Indeed made of neutrons (mostly, typically 8 n every p^+ / e^-) – sustained by the pressure of degenerate neutrons
 - Fast rotators
 - $P \approx 10^{-2} - 10 \text{ s}$
 - $\dot{P} \approx 10^{-20} - 10^{-9} \text{ s/s}$



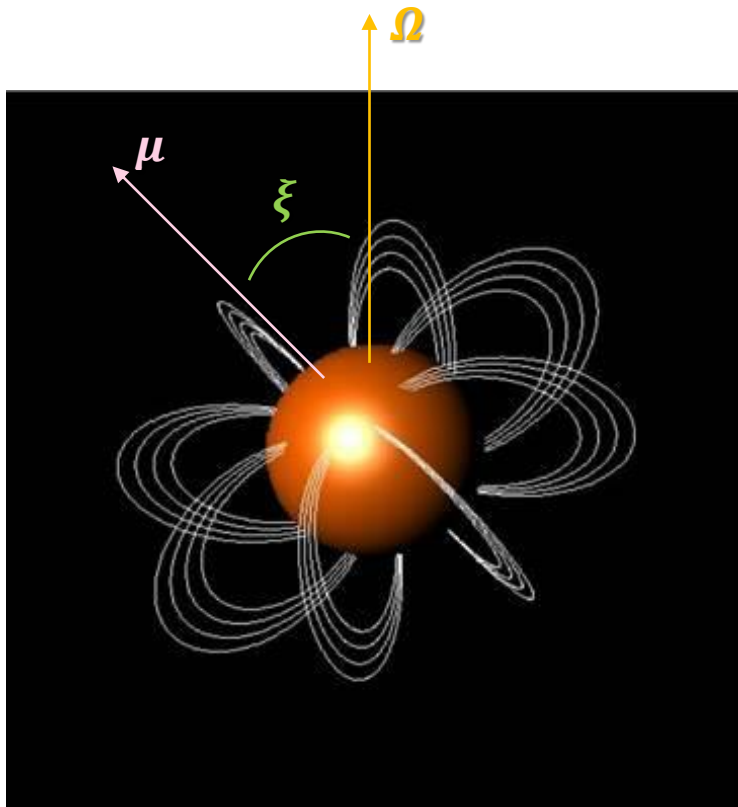
Neutron stars: general notions

- Neutron stars (NSs) are relics of massive stars ($M_{\text{prog}} \approx 8 - 25 M_{\odot}$)
 - Masses $M_{\text{NS}} \approx 1 - 2 M_{\odot}$
 - Radii $R_{\text{NS}} \approx 10 - 15 \text{ km}$
- } $\rho_{\text{m}} \approx 10^{14} - 10^{15} \text{ g/cm}^3$
- Indeed made of neutrons (mostly, typically 8 n every p^+ / e^-) – sustained by the pressure of degenerate neutrons
 - Fast rotators
 - Powerful magnets



Magneto-rotational evolution

- A rotating dipole field emits EM radiation at the expenses of the rotational energy



Larmor formula

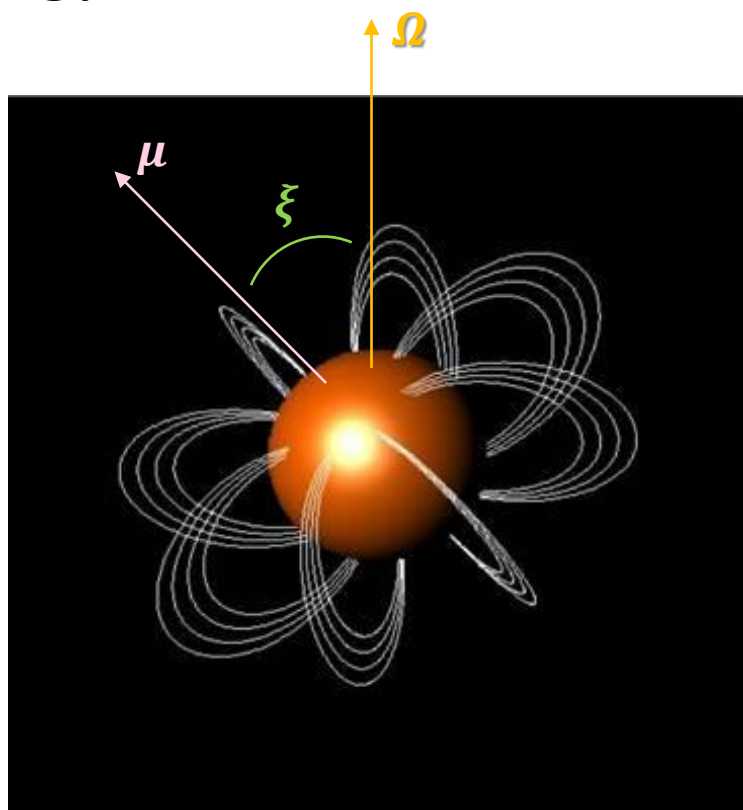
$$-\frac{2}{3c^3} \left(\frac{\partial^2 \mu}{\partial t^2} \right)^2 = I\Omega\dot{\Omega}$$

Magnetic dipole moment

Rotation frequency
($\Omega = 2\pi/P$)

Magneto-rotational evolution

- A rotating dipole field emits EM radiation at the expenses of the rotational energy



Solving for B

$$B \approx 3.2 \times 10^{19} \sqrt{P\dot{P}} \text{ G}$$

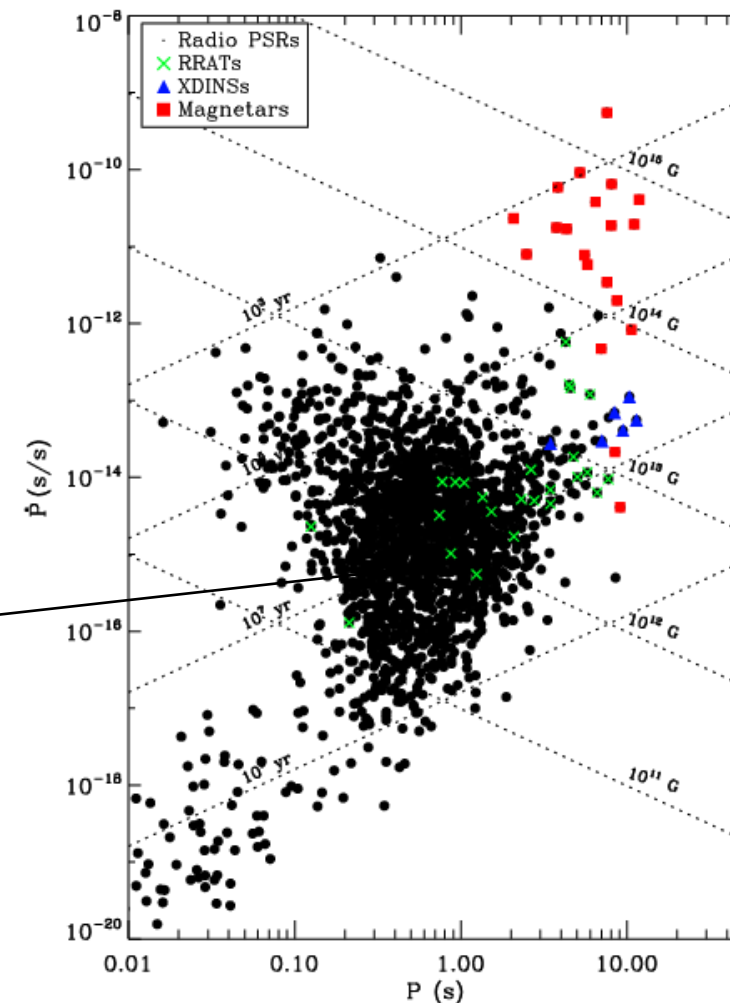


This holds for:

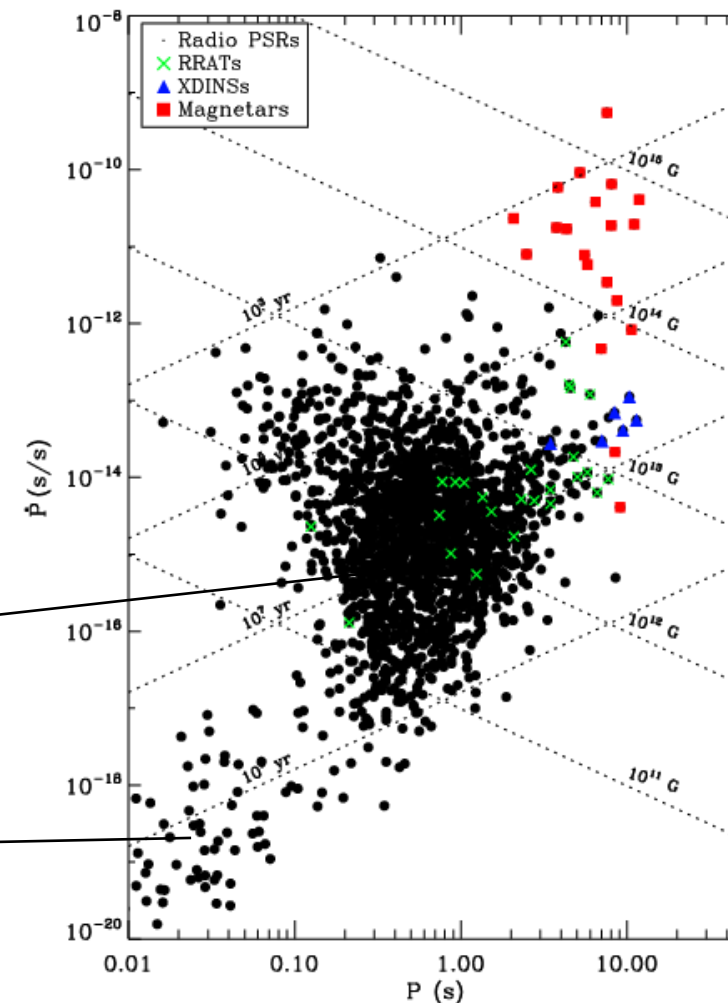
- purely dipolar magnetic field (μ in the Larmor formula)
- all the rotation energy is converted into EM emission

- Classification of NSs according to their values of P and \dot{P}

Rotation-Powered Pulsars (RPPs)



- Classification of NSs according to their values of P and \dot{P}



Rotation-Powered Pulsars (RPPs)

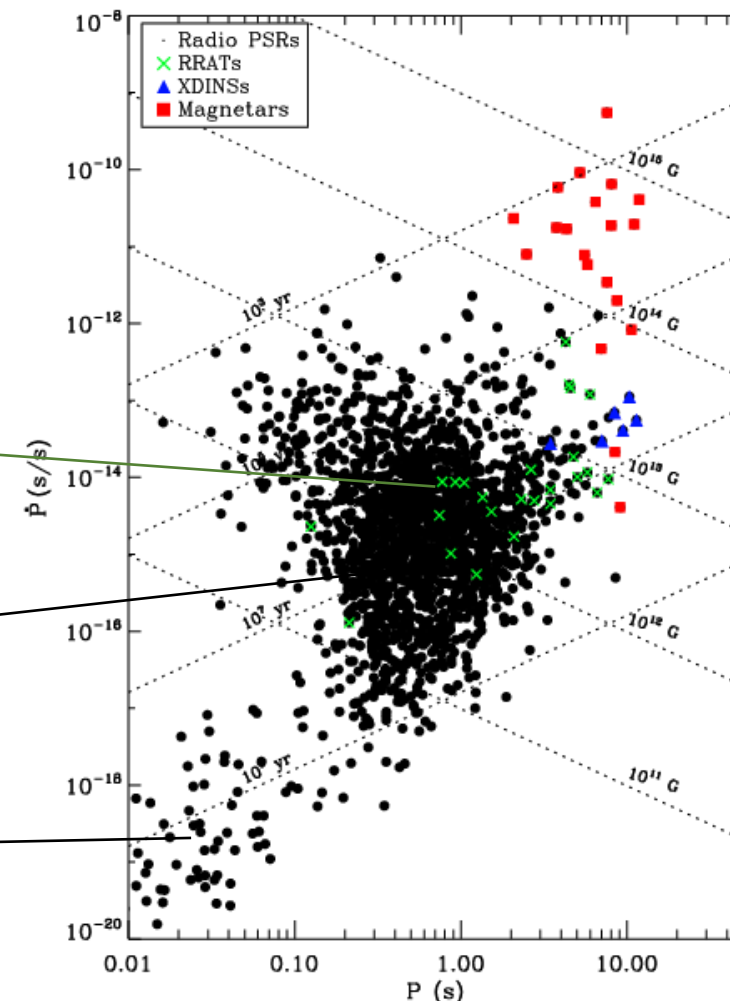
(Accreting) millisecond pulsars

- Classification of NSs according to their values of P and \dot{P}

Rotating Radio Transients (RRaTs)

Rotation-Powered Pulsars (RPPs)

(Accreting) millisecond pulsars



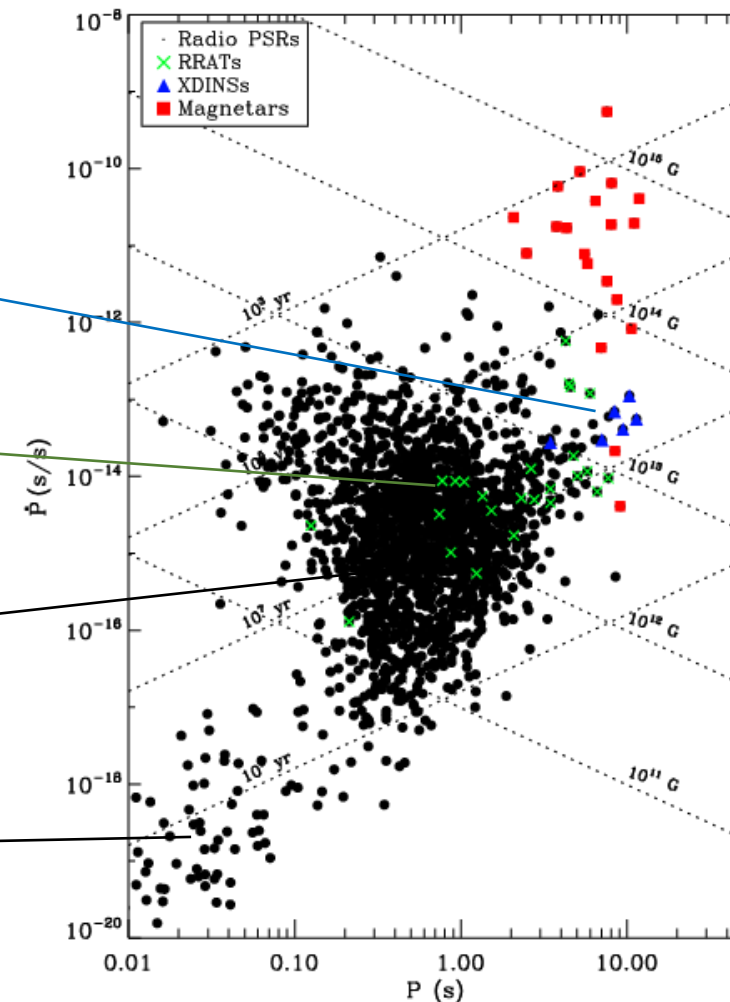
- Classification of NSs according to their values of P and \dot{P}

X-ray Dim Isolated NSs (XDINSSs)

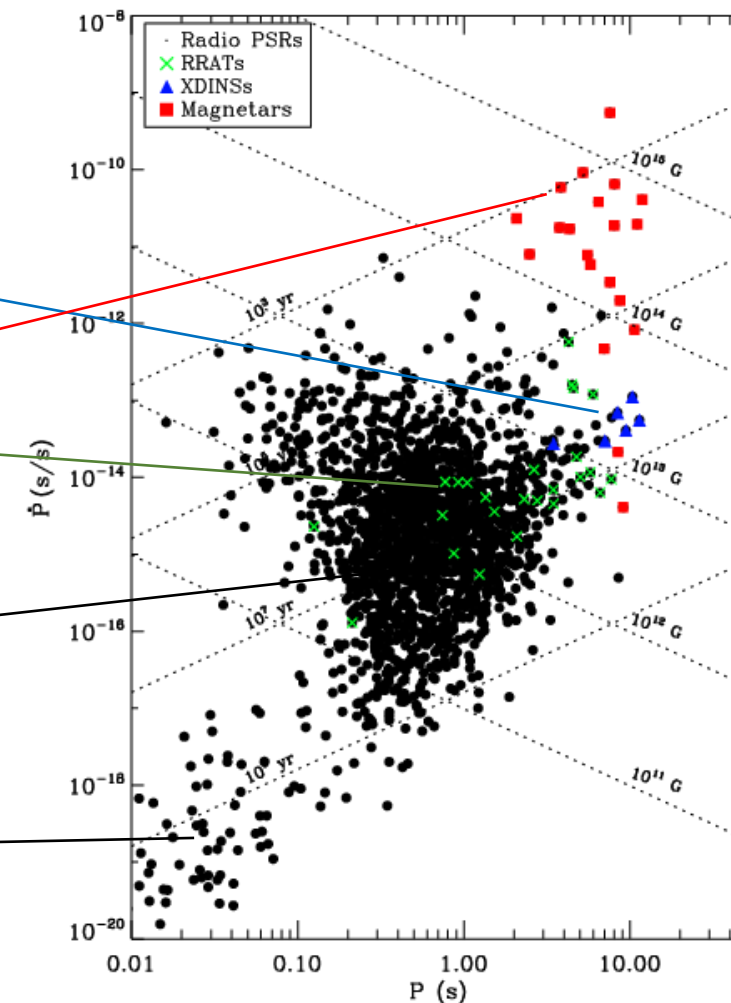
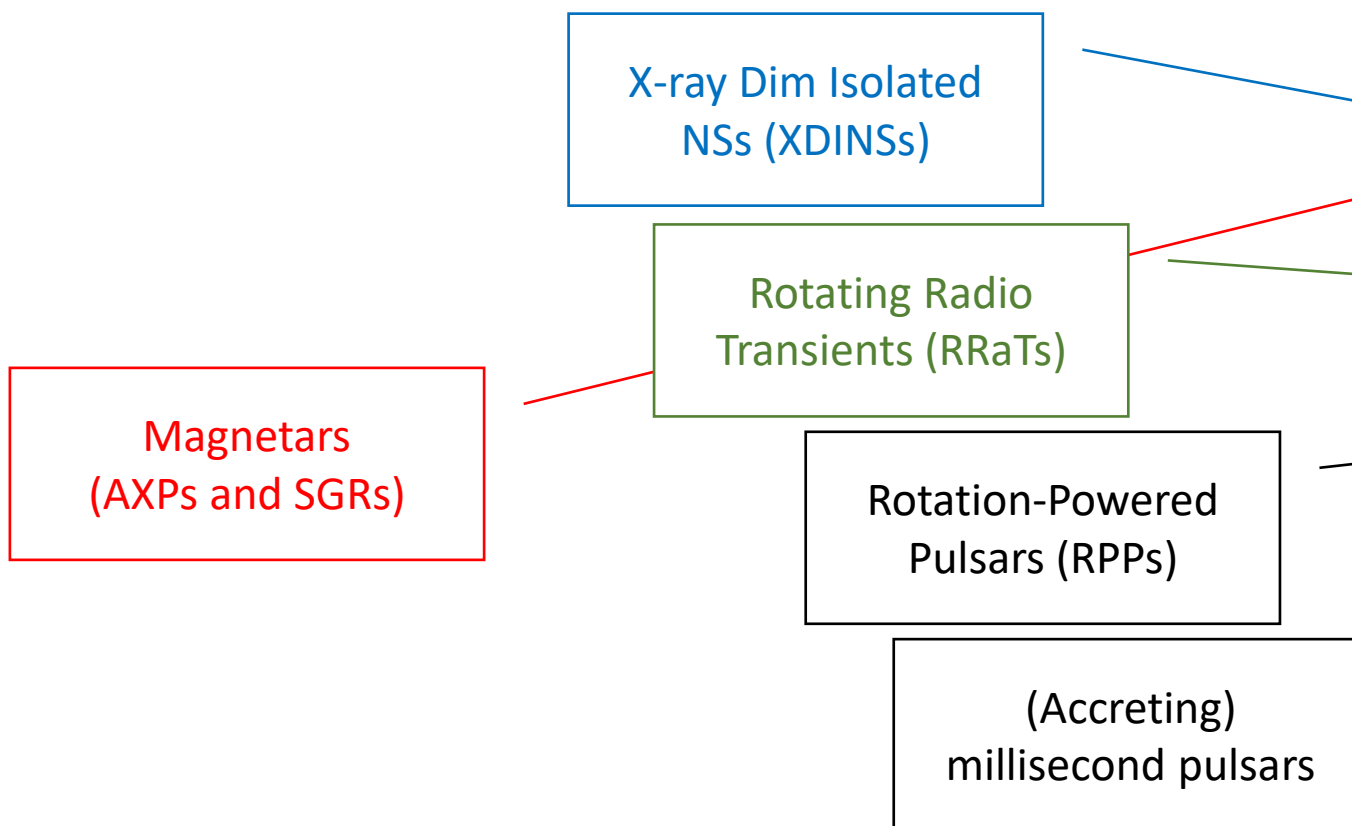
Rotating Radio Transients (RRaTs)

Rotation-Powered Pulsars (RPPs)

(Accreting) millisecond pulsars

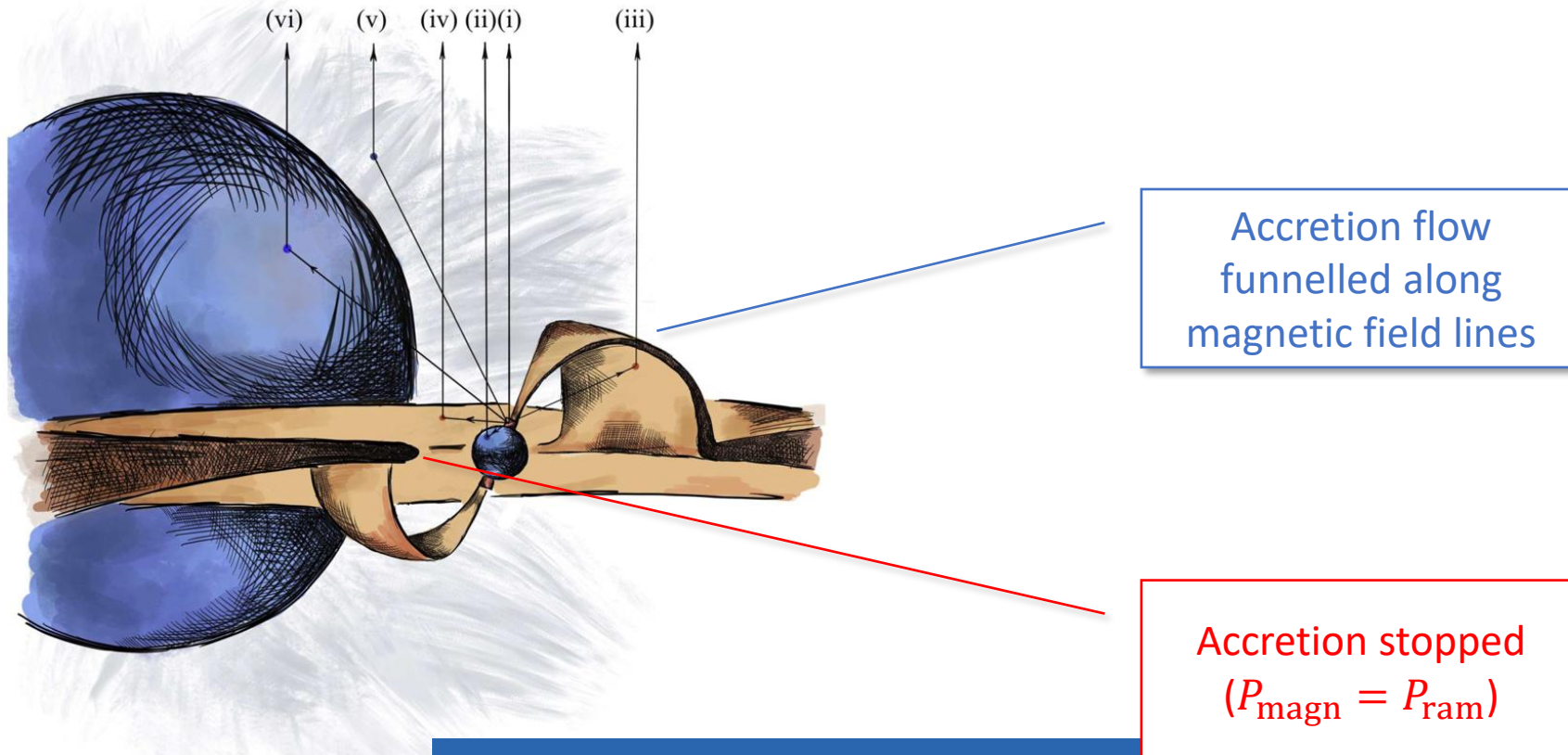


- Classification of NSs according to their values of P and \dot{P}



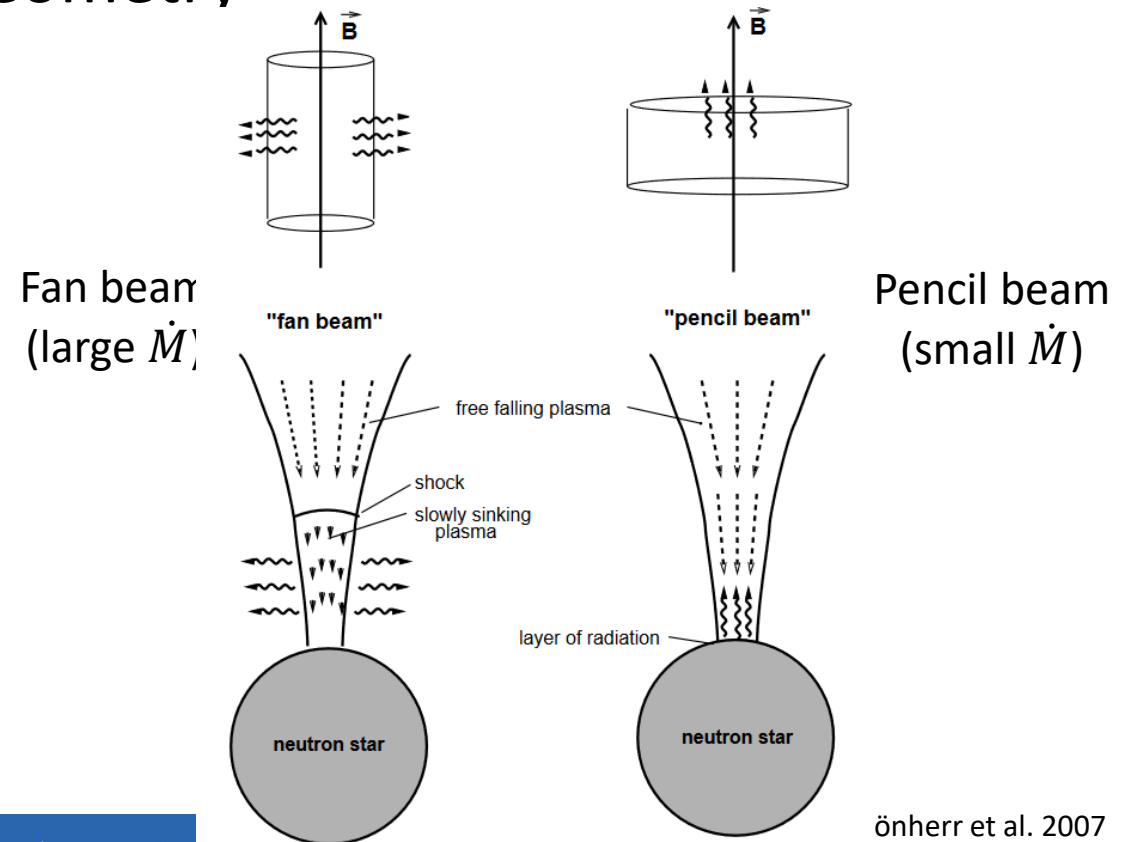
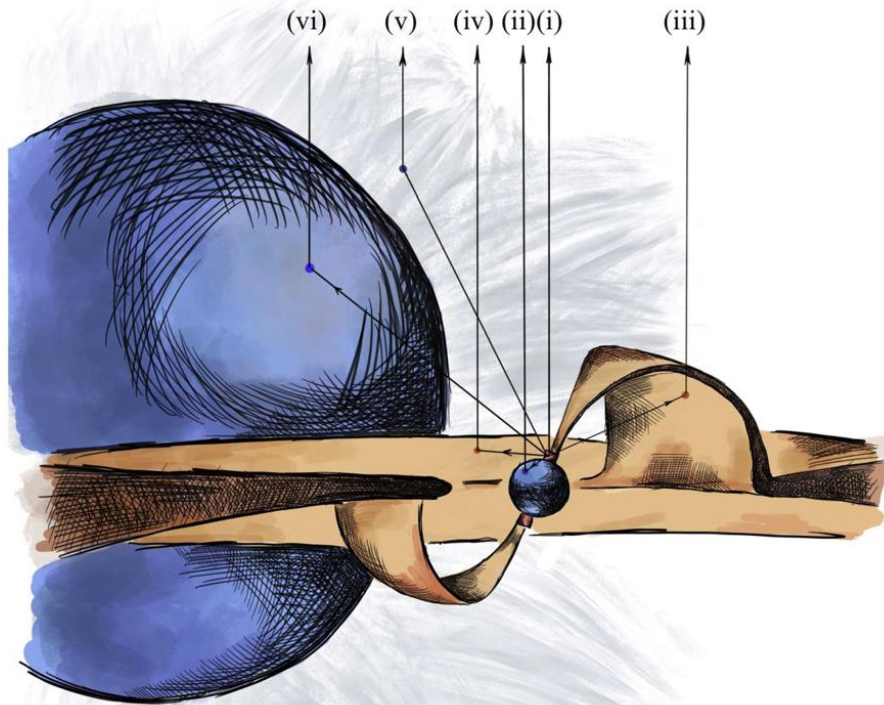
Accreting X-ray pulsars (XRPs)

- Strongly magnetized NSs ($B \approx 10^{12-13}$ G) in binary systems
- Emission determined by accretion geometry



Accreting X-ray pulsars (XRPs)

- Strongly magnetized NSs ($B \approx 10^{12-13}$ G) in binary systems
- Emission determined by accretion geometry

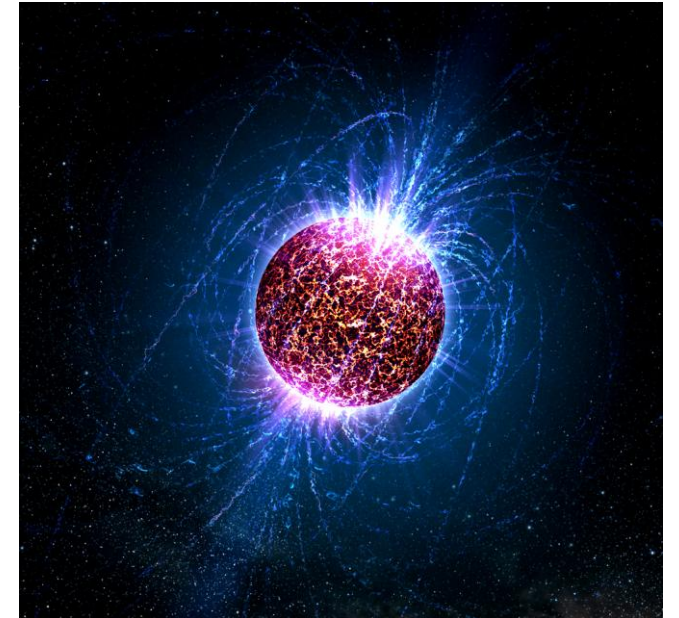
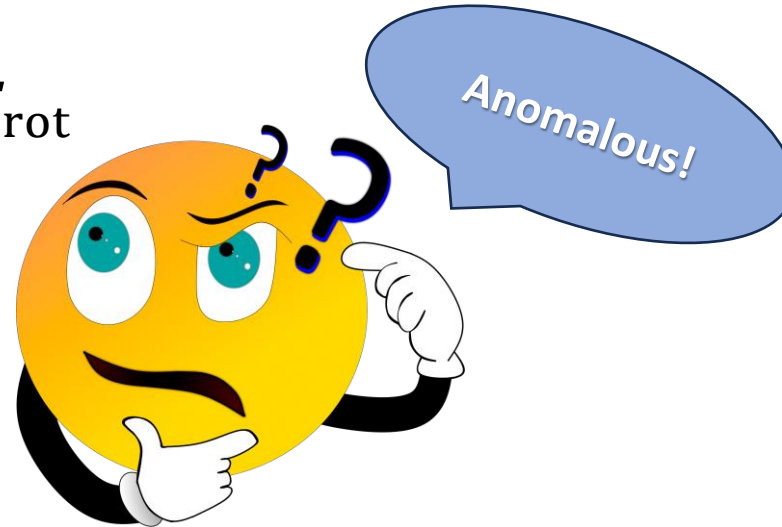


öherr et al. 2007

Anomalous X-ray pulsars (AXPs)

- Isolated NSs
- X-ray luminosity (usually) in excess of the rotational energy loss rate

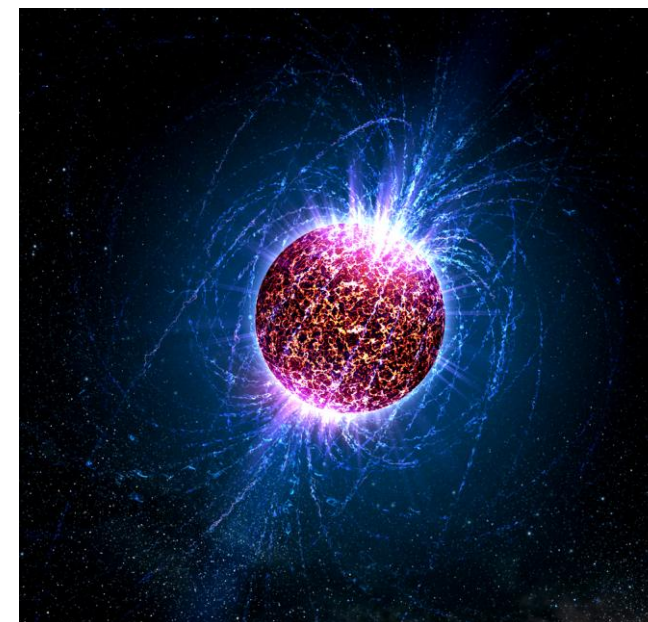
$$L_X > \dot{E}_{\text{rot}}$$



Anomalous X-ray pulsars (AXPs)

- Isolated NSs
- X-ray luminosity (usually) in excess of the rotational energy loss rate
- Large spin periods and spin-down rates

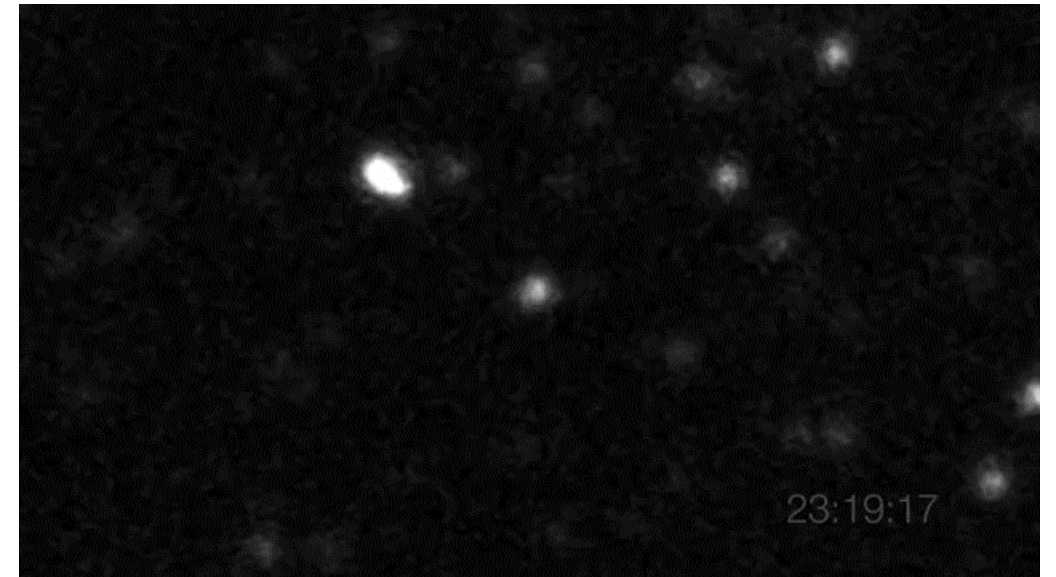
$$P \approx 2 - 12 \text{ s} \quad \Rightarrow \quad B_{\text{sd}} \approx 10^{14} - 10^{15} \text{ G}$$
$$\dot{P} \approx 10^{-13} - 10^{-9} \text{ s/s}$$



Ultra strong!

Soft- γ repeaters (SGRs)

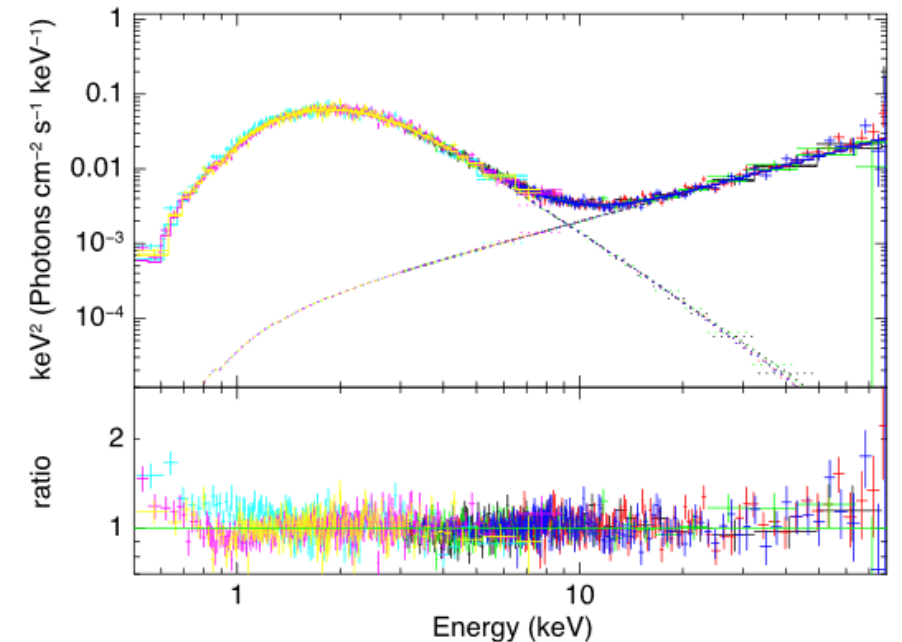
- Sudden emission of a huge amount of X-ray energy (up to 10^{47} erg/s)
- Initially confused with GRBs (but then observed to repeat)
- Pulsations detected in the event afterglow (\rightarrow NSs!)
- P and \dot{P} compatible with those of AXPs (and so again $B_{sd} \approx 10^{14-15}$ G)
- Still isolated objects



A.J. Castro-Tirado/IAC80/ESO

Magnetars – Persistent emission

- Properties of AXPs and SGRs are shared between the two classes
- Energy must be supplied by the ultra-strong magnetic field (MAGNETic stARs)
- Persistent and transient sources
- Soft X-ray persistent spectra (0.5 – 10 keV) are usually fitted by a BB+PL decomposition (BB+BB for transients)
- Additional PL component at higher energies ($\gtrsim 20$ keV)



Tendulkar et al. (2015)

Magnetars – Bursting activity

- Short bursts

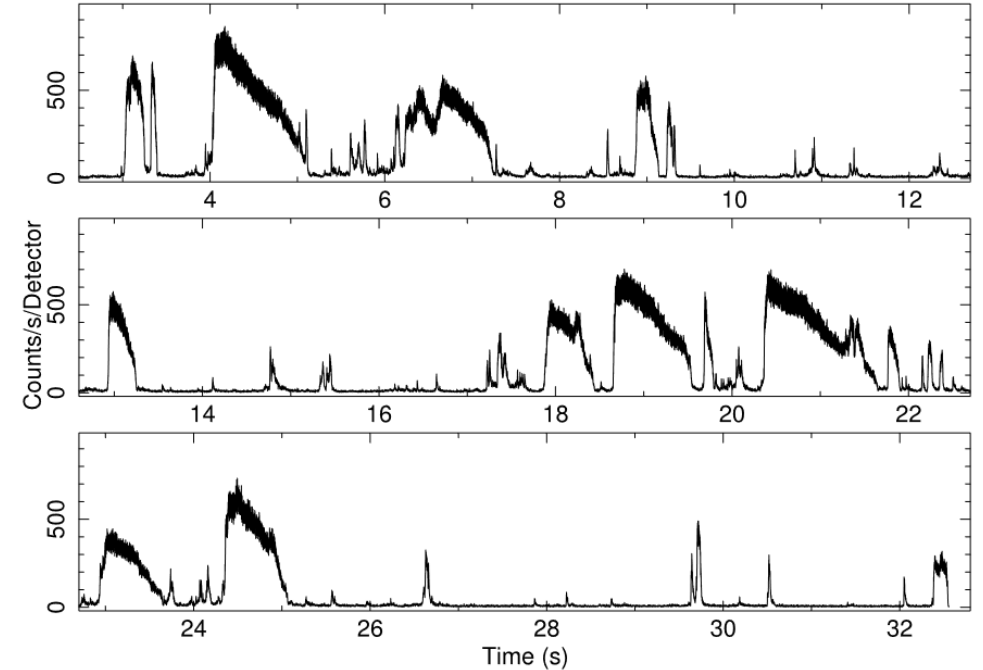
- $\Delta t \approx 0.01 - 1 \text{ s}$
- $L_X \approx 10^{36} - 10^{41} \text{ erg/s}$

- (Intermediate) flares

- $\Delta t \approx 1 - 10 \text{ s}$
- $L_X \approx 10^{41} - 10^{43} \text{ erg/s}$

- Giant flares

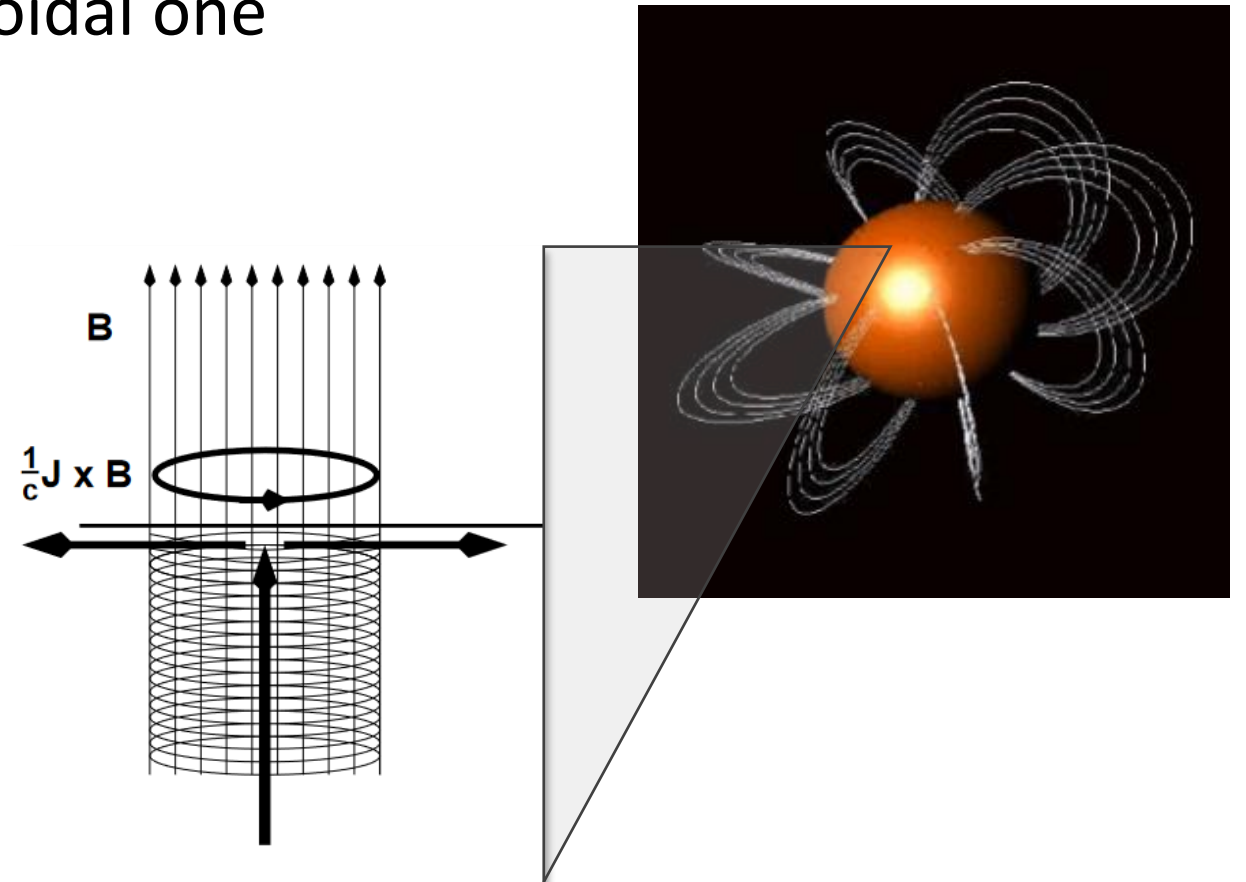
- $\Delta t \approx 10^2 \text{ s}$
- $L_X \approx 10^{44} - 10^{47} \text{ erg/s}$



Israel et al. (2008)

Twisted-magnetosphere scenario

- The strong internal field (up to 10^{16} G) must contain a toroidal component at least of the same order of the poloidal one



Twisted-magnetosphere scenario

- The strong internal field (up to 10^{16} G) must contain a toroidal component at least of the same order of the poloidal one
- Once the magnetic stress exceeds the crust mechanical yield, helicity is transferred to the external field

dipole

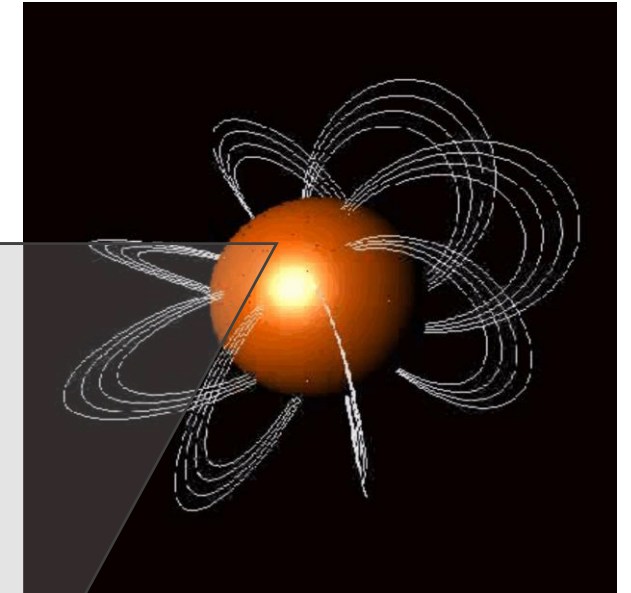
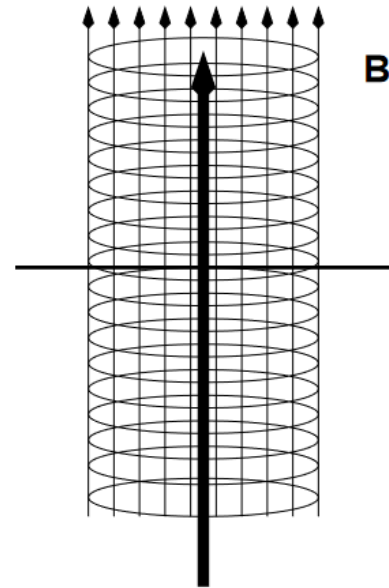
$$\mathbf{B} = [B_r, B_\theta, B_\phi] = \frac{B_p}{2} \left(\frac{R_{NS}}{r} \right)^3 [2 \cos \theta, \sin \theta, 0]$$



twisted dipole

$$\mathbf{B} = \frac{B_p}{2} \left(\frac{R_{NS}}{r} \right)^{2+p} \left[-\frac{df}{d \cos \theta}, \frac{pf}{\sin \theta}, \sqrt{\frac{pC(p)}{p+1}} \frac{f^{1+1/p}}{\sin \theta} \right]$$

$$0 < p \leq 1$$

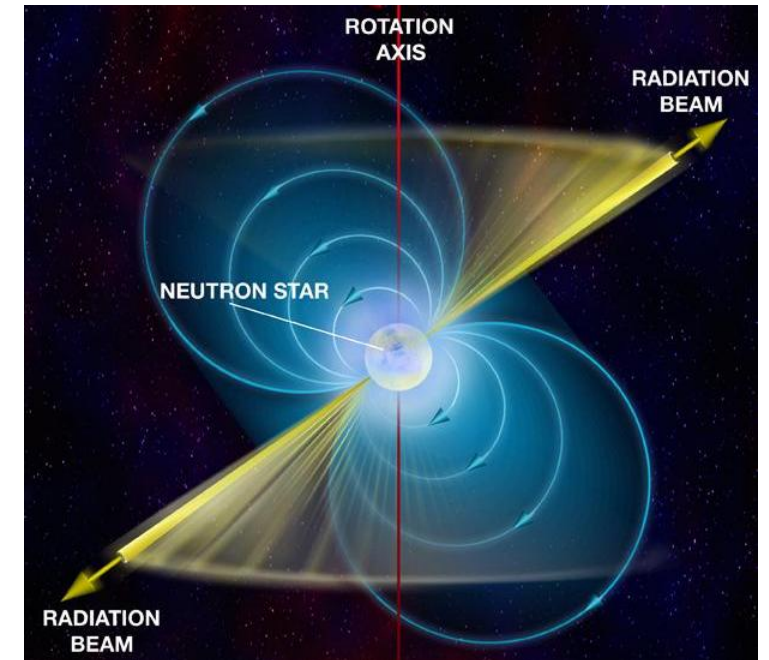


Twisted-magnetosphere scenario

$$\nabla \times \mathbf{B}_{\text{dip}} = 4\pi\mathbf{j}/c$$

|| ↓

$$0 \quad \text{no currents}$$



Twisted-magnetosphere scenario

$$\nabla \times \mathbf{B}_{\text{dip}} = 4\pi\mathbf{j}/c$$

||

0

no currents

⇓

$$\nabla \times \mathbf{B}_{\text{twist}} = 4\pi\mathbf{j}/c$$

≠

0

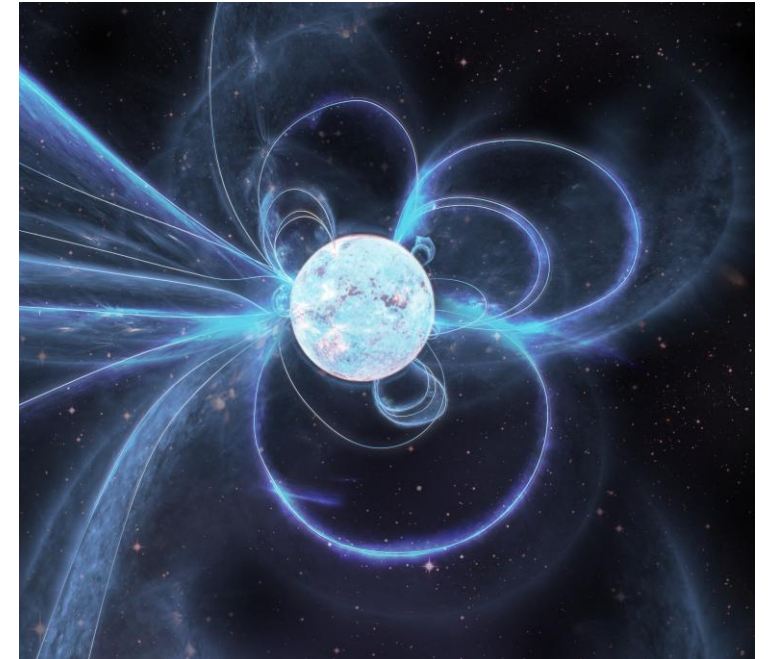
currents

⇓

- Magnetosphere is populated by charged particles:

$$n_e \sim \frac{B}{r\beta} \left(\frac{B_\phi}{B_\theta} \right)$$

not enough for photons to interact efficiently



Twisted-magnetosphere scenario

$$\nabla \times \mathbf{B}_{\text{dip}} = 4\pi\mathbf{j}/c$$

\parallel
 \Downarrow
 0 no currents

$$\nabla \times \mathbf{B}_{\text{twist}} = 4\pi\mathbf{j}/c$$

\nparallel
 \Downarrow
 0 **currents**

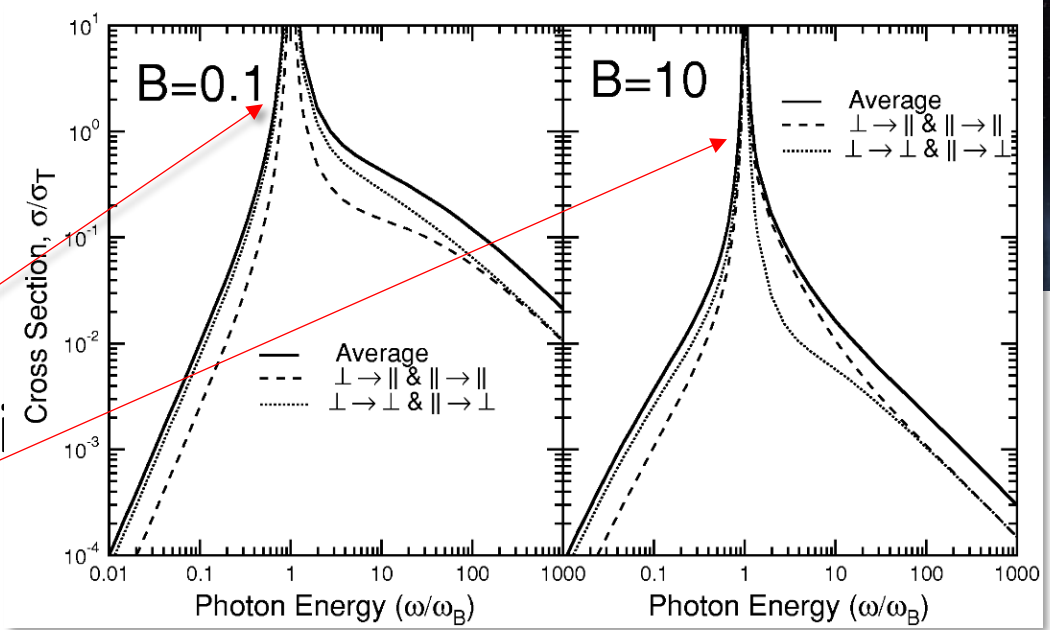


- Magnetosphere is populated by charged

$$n_e \sim \frac{B}{r\beta} \left(\frac{B_\phi}{B_\theta} \right)$$

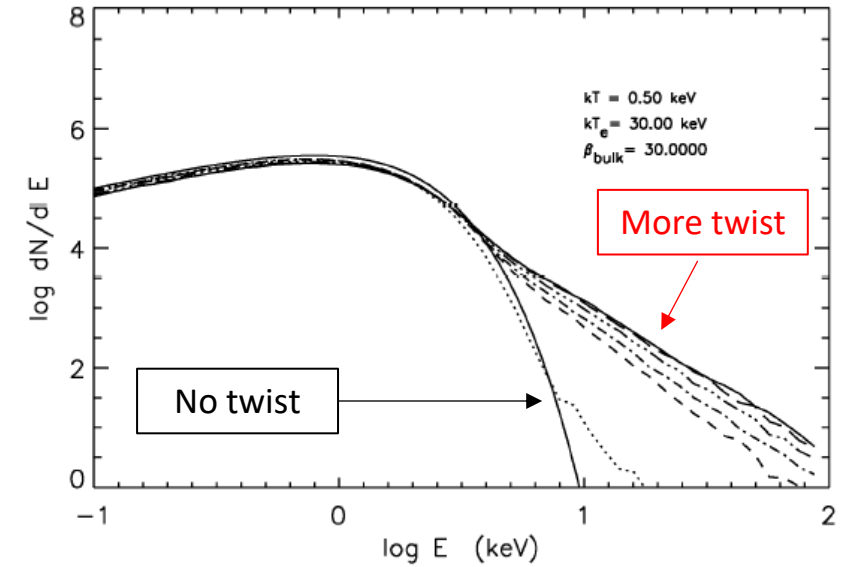
not enough for photons to interact efficiently

Scattering cross sections peak at the cyclotron energy



Magnetar model achievements (till IXPE)

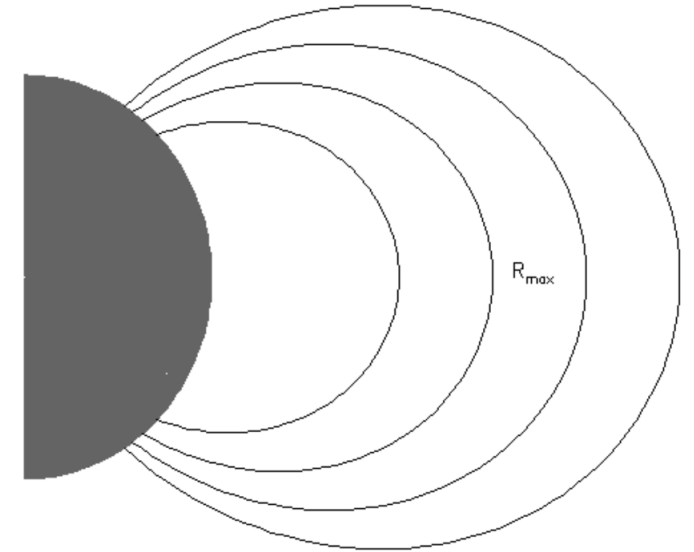
- RCS of thermal photons onto magnetospheric particles generates PL tails at soft X-ray energies



Nobili et al. (2008)

Magnetar model achievements (till IXPE)

- RCS of thermal photons onto magnetospheric particles generates PL tails at soft X-ray energies
- Internal magnetic stresses on the star crust induce injection of e^-e^+ magnetically confined fireball (at the base of burst emission)
- Magnetic scattering models can explain the observed spectral properties



Magnetar model alternatives

- The $P-\dot{P}$ estimate of the magnetic field strength holds for:
 - dipolar fields (magnetar field topology not dipolar)
 - emission energy all supplied by rotation (need for another source of energy)
- Magnetar phenomenology very different from other NSs
 - strongly-magnetized ($\approx 10^9$ G) white dwarfs?
 - disrupting events for SGRs?

May polarimetry provide new constraints?

Polarization in strongly magnetized environments

- The polarization state of photons can be studied solving the wave equation

$$\nabla \times (\bar{\mu} \cdot \nabla \times \mathbf{E}) = \frac{\omega^2}{c^2} \epsilon \cdot \mathbf{E}$$

magnetic permeability
tensor (inverse)

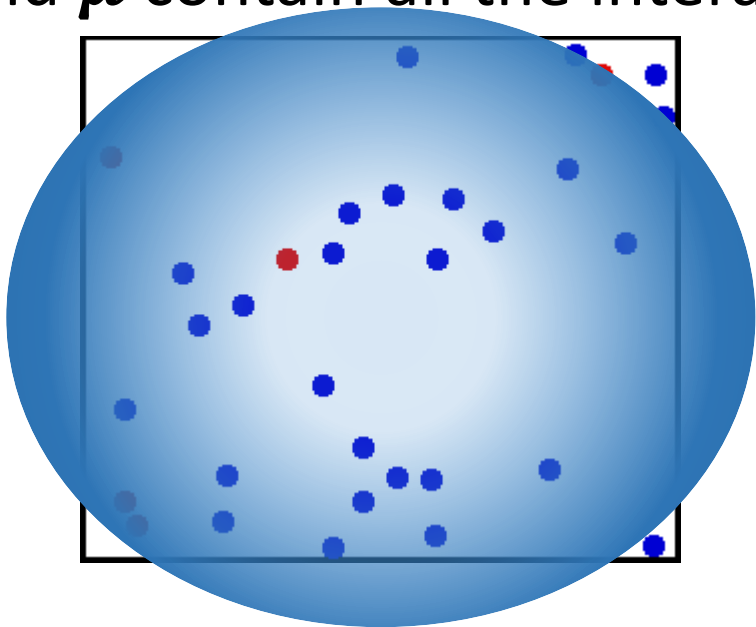
dielectric tensor

Polarization in strongly magnetized environments

- The polarization state of photons can be studied solving the wave equation

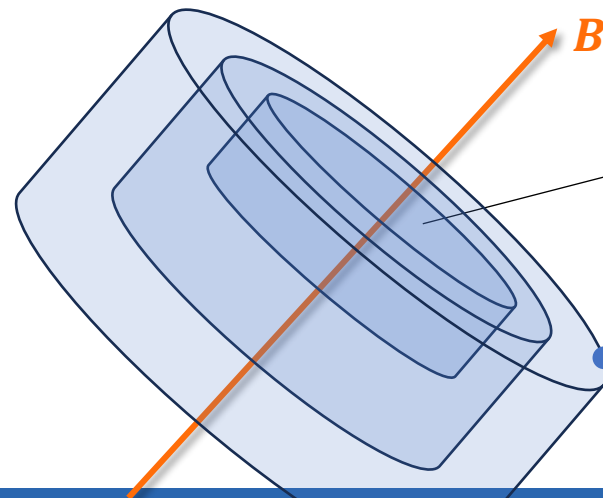
$$\nabla \times (\bar{\mu} \cdot \nabla \times \mathbf{E}) = \frac{\omega^2}{c^2} \epsilon \cdot \mathbf{E}$$

- ϵ and $\bar{\mu}$ contain all the interaction terms



magnetized plasma

In strong B fields the charge motion is quantized



1st Landau level energy

$$\hbar\omega_B = \frac{\hbar e B_Q}{m_e c} = m_e c^2$$

↓

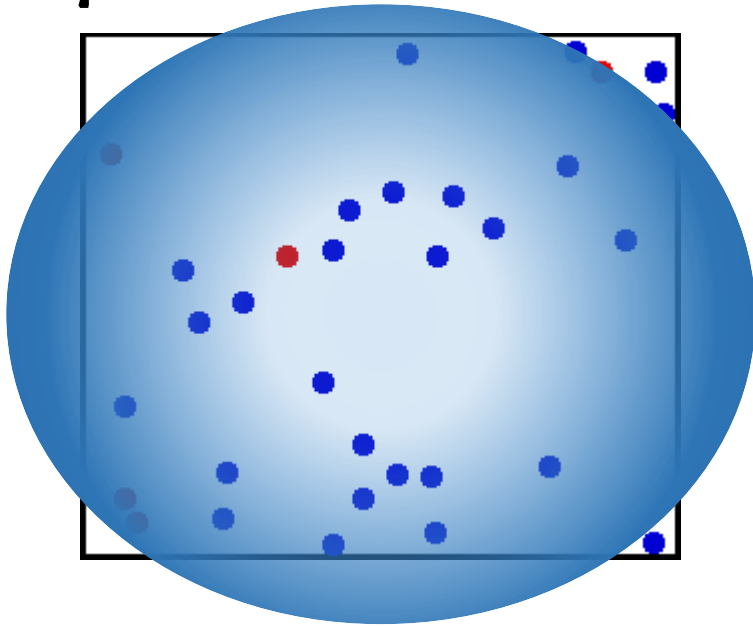
$$B_Q = \frac{m_e^2 c^3}{\hbar e} = 4.414 \times 10^{13} \text{ G}$$

Polarization in strongly magnetized environments

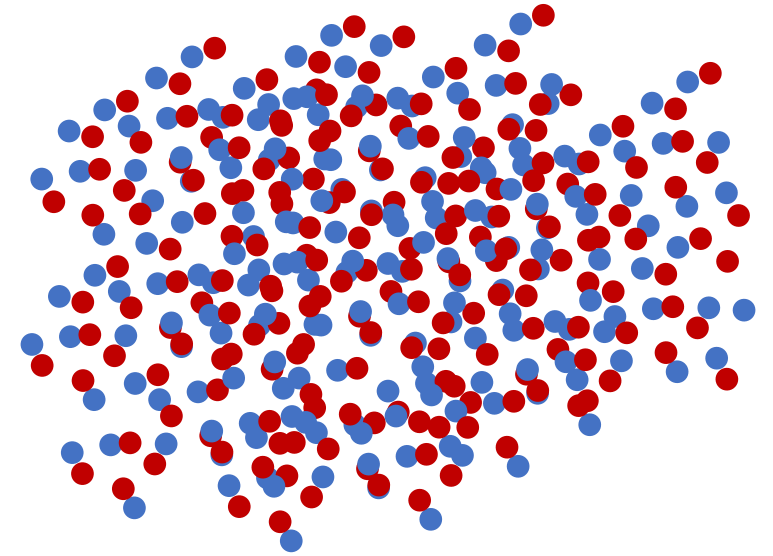
- The polarization state of photons can be studied solving the wave equation

$$\nabla \times (\bar{\mu} \cdot \nabla \times \mathbf{E}) = \frac{\omega^2}{c^2} \epsilon \cdot \mathbf{E}$$

- ϵ and $\bar{\mu}$ contain all the interaction terms



magnetized plasma



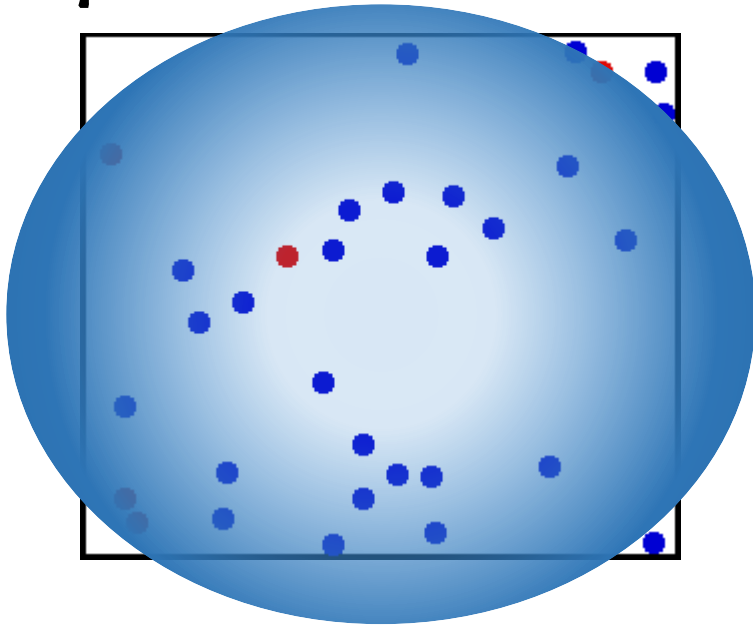
vacuum birefringence

Polarization in strongly magnetized environments

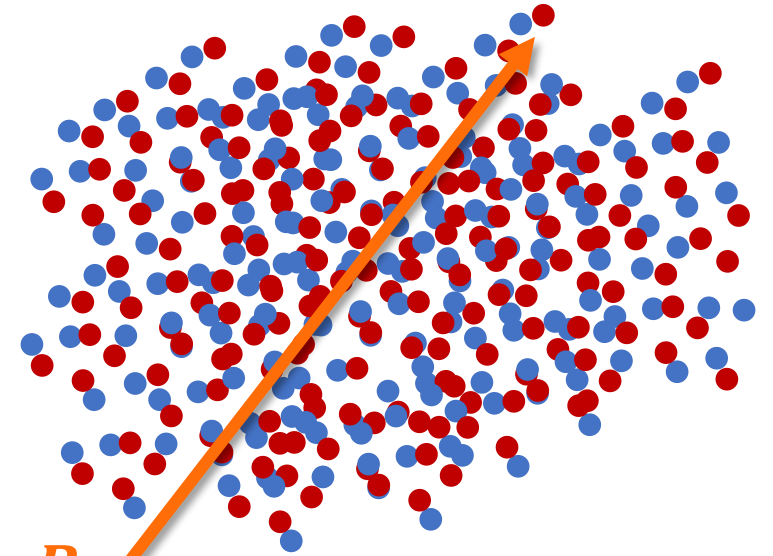
- The polarization state of photons can be studied solving the wave equation

$$\nabla \times (\bar{\mu} \cdot \nabla \times \mathbf{E}) = \frac{\omega^2}{c^2} \epsilon \cdot \mathbf{E}$$

- ϵ and $\bar{\mu}$ contain all the interaction terms



magnetized plasma



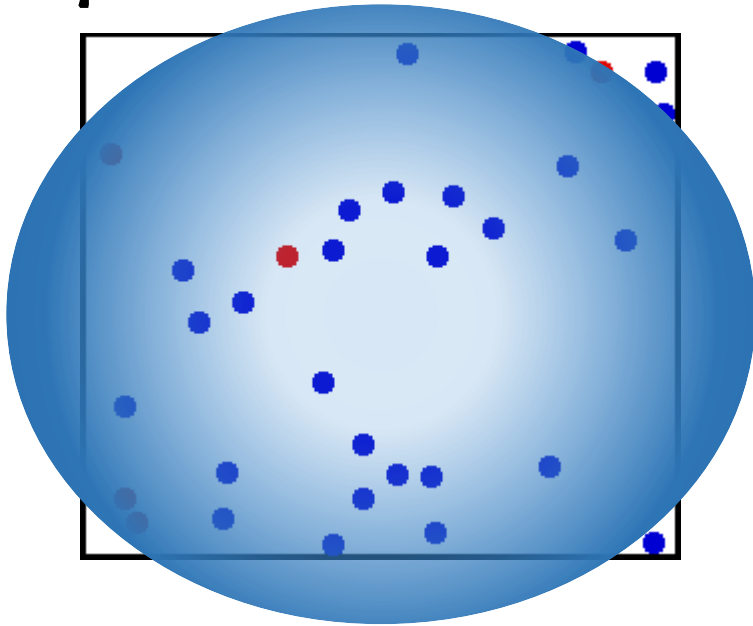
B vacuum birefringence

Polarization in strongly magnetized environments

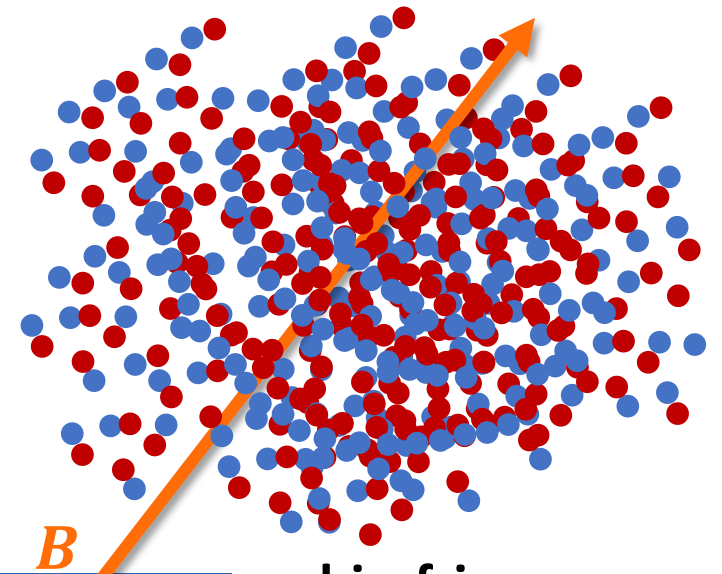
- The polarization state of photons can be studied solving the wave equation

$$\nabla \times (\bar{\mu} \cdot \nabla \times \mathbf{E}) = \frac{\omega^2}{c^2} \epsilon \cdot \mathbf{E}$$

- ϵ and $\bar{\mu}$ contain all the interaction terms



magnetized plasma



B vacuum birefringence

Polarization in strongly magnetized environments

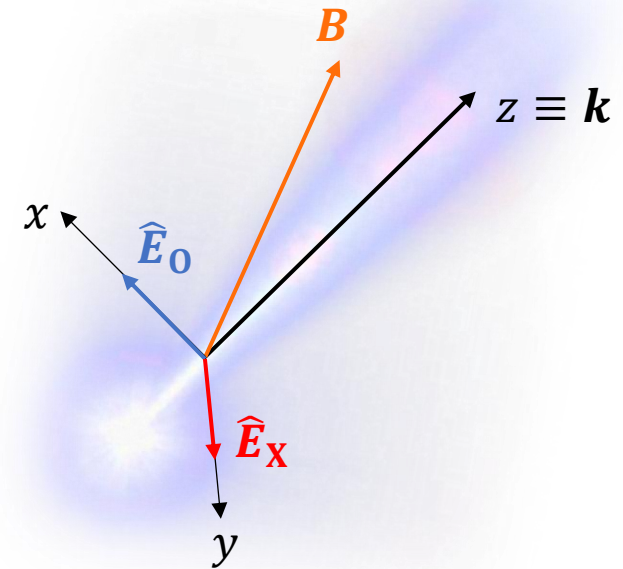
- The polarization state of photons can be studied solving the wave equation

$$\nabla \times (\bar{\mu} \cdot \nabla \times \mathbf{E}) = \frac{\omega^2}{c^2} \epsilon \cdot \mathbf{E}$$

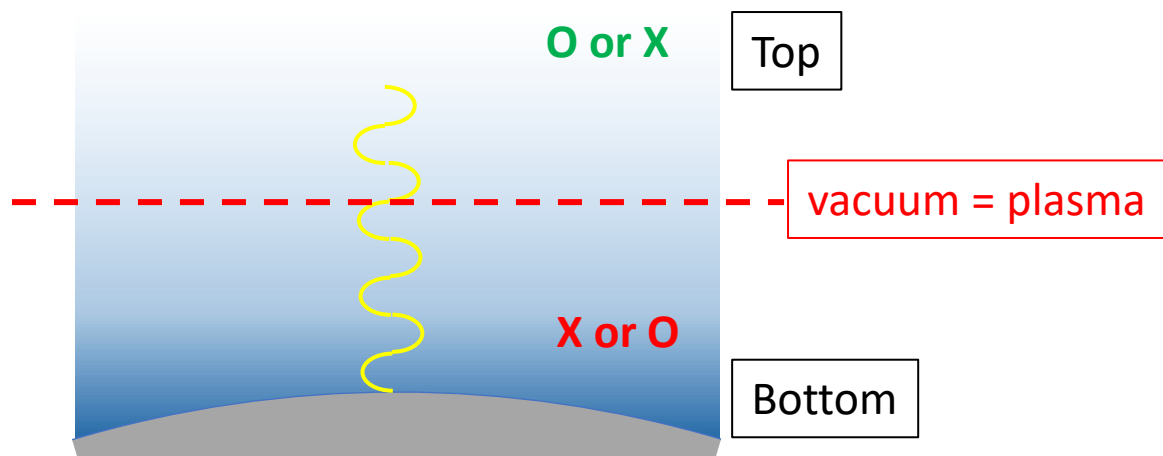
- ϵ and $\bar{\mu}$ contain all the interaction terms
- Either with plasma or vacuum dominating

$$\hat{\mathbf{E}} = \begin{pmatrix} 1 \\ 0 \\ 0 \end{pmatrix} \quad \text{or} \quad \begin{pmatrix} 0 \\ 1 \\ 0 \end{pmatrix}$$

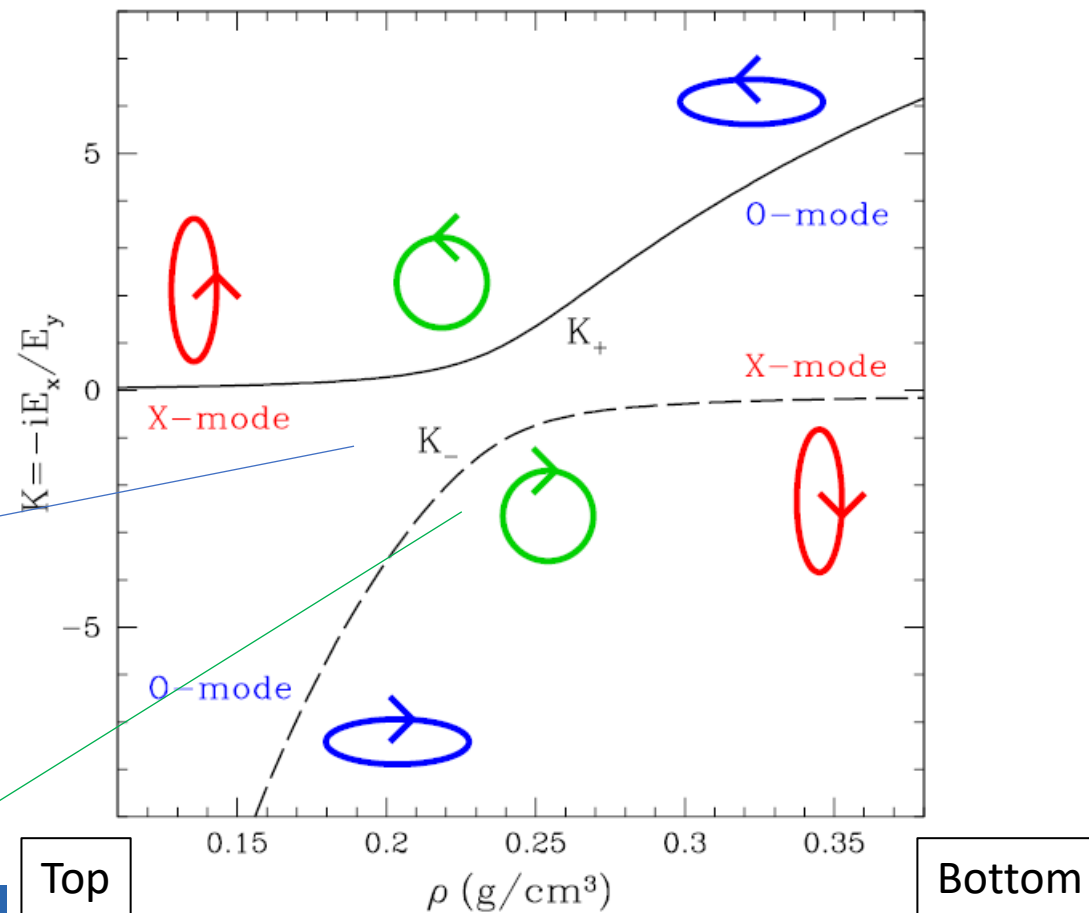
Ordinary mode Extraordinary mode



- Plasma and vacuum contributions balance at a given density



Mode conversion



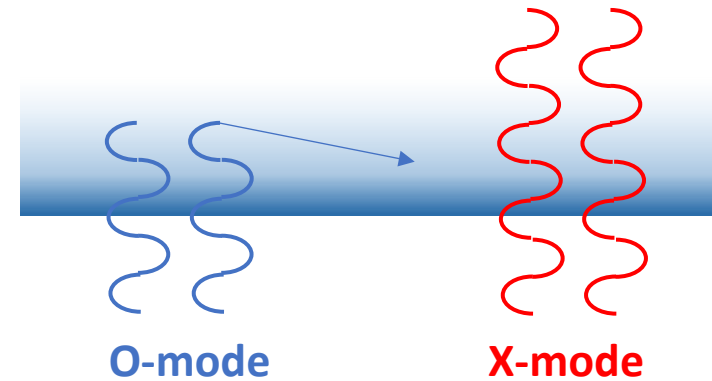
Circular polarization

Dichroism in strongly-magnetized plasma

- In strong fields ($B \gtrsim B_Q$) plasma is (generally) transparent for X-photons

$$\sigma_{OO} \sim \sigma_{\text{unmag}} \quad \sigma_{XO} \sim \left(\frac{B}{B_Q}\right)^{-2} \sigma_{OO}$$

$$\sigma_{OX} \sim \left(\frac{B}{B_Q}\right)^{-2} \sigma_{OO} \quad \sigma_{XX} \sim \left(\frac{B}{B_Q}\right)^{-2} \sigma_{OO}$$



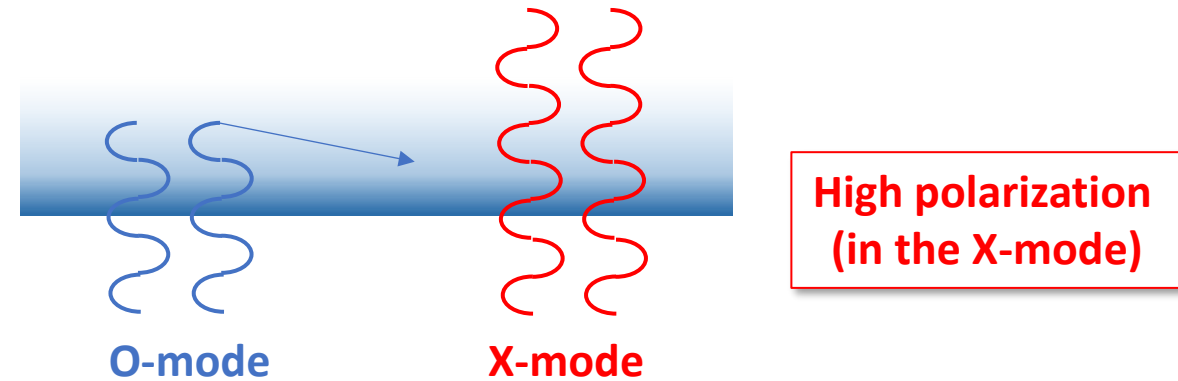
**High polarization
(in the X-mode)**

Dichroism in strongly-magnetized plasma

- In strong fields ($B \gtrsim B_Q$) plasma is (generally) transparent for X-photons

$$\sigma_{OO} \sim \sigma_{\text{unmag}} \quad \sigma_{XO} \sim \left(\frac{B}{B_Q}\right)^{-2} \sigma_{OO}$$

$$\sigma_{OX} \sim \left(\frac{B}{B_Q}\right)^{-2} \sigma_{OO} \quad \sigma_{XX} \sim \left(\frac{B}{B_Q}\right)^{-2} \sigma_{OO}$$



- At the cyclotron resonance:

$$\sigma_{OO} = \frac{1}{3} \sigma_{OX} \quad \sigma_{XX} = 3\sigma_{XO}$$

- X-mode photons are still preferred, but emerging radiation is only 33% polarized

Propagation in the pure magnetized vacuum

- Solving the wave equation accounting for vacuum effects only yields

$$\frac{2}{k_0 \delta} \frac{dE_x}{dz} = i [M E_x + P E_y] \quad \frac{2}{k_0 \delta} \frac{dE_y}{dz} = i [P E_x + N E_y]$$

$$\delta \sim (B/B_Q)^2$$

Propagation in the pure magnetized vacuum

- Solving the wave equation accounting for vacuum effects only it reduces to

$$\frac{2}{k_0 \delta} \frac{dE_x}{dz} = i [ME_x + PE_y]$$

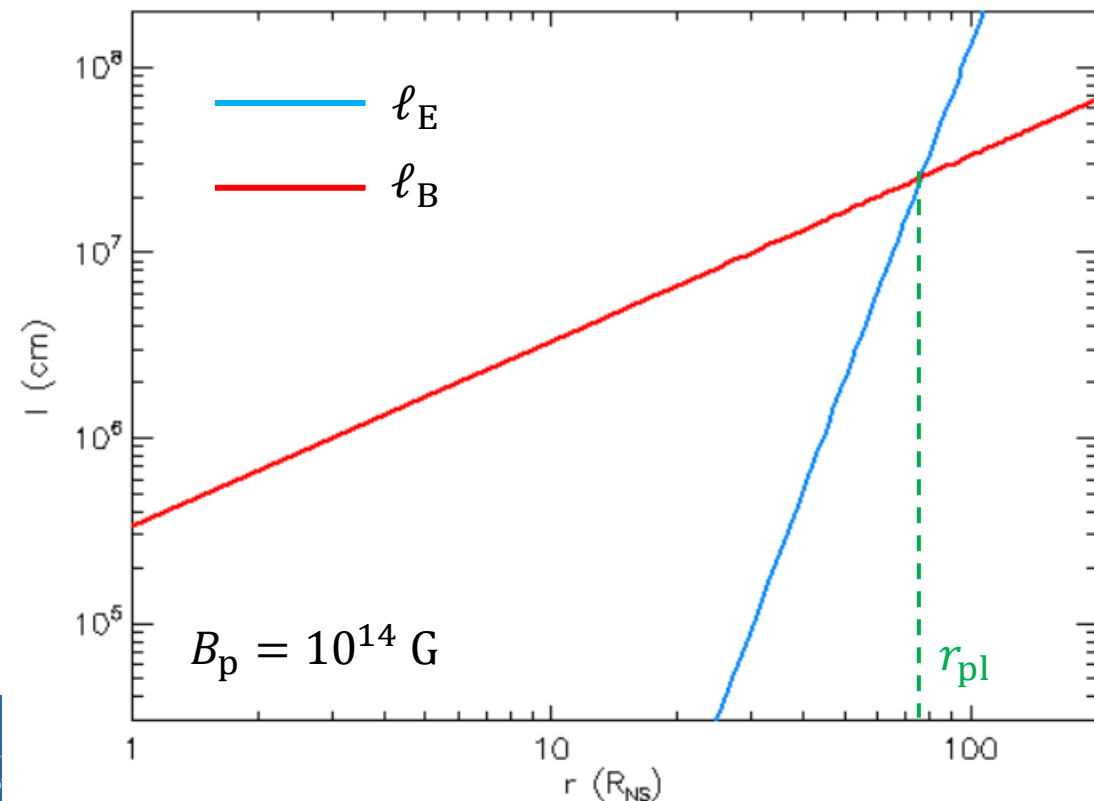
$$\frac{2}{k_0 \delta} \frac{dE_y}{dz} = i [PE_x + NE_y]$$

E-field evolution length:

$$\ell_E = \frac{2}{k_0 \delta} \approx 130 \left(\frac{B}{10^{11} \text{ G}} \right)^{-2} \left(\frac{\hbar \omega}{1 \text{ keV}} \right)^{-1} \text{ cm}$$

(Dipolar) *B*-field evolution length:

$$\ell_B = \frac{B}{|\mathbf{k} \cdot \nabla B|} \approx \frac{r}{3}$$



Propagation in the pure magnetized vacuum

- Solving the wave equation accounting for vacuum effects only it reduces to

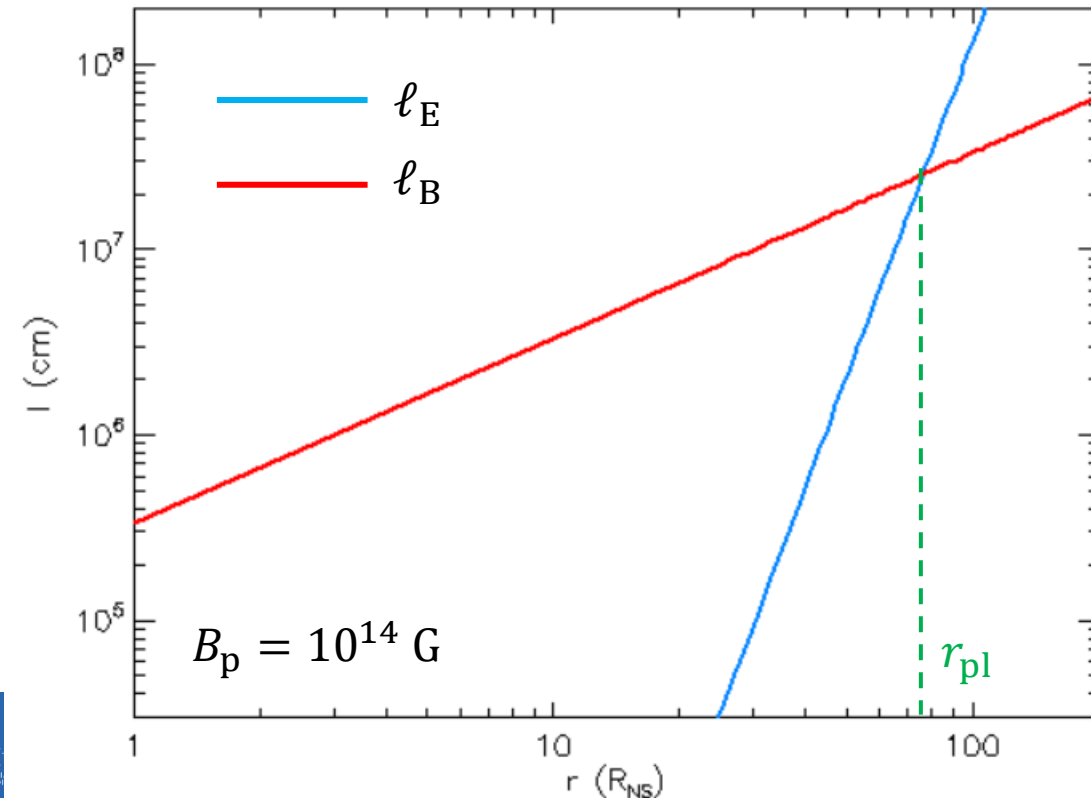
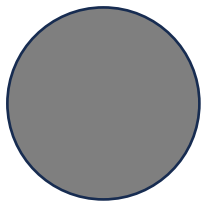
$$\frac{2}{k_0 \delta} \frac{dE_x}{dz} = i [ME_x + PE_y]$$

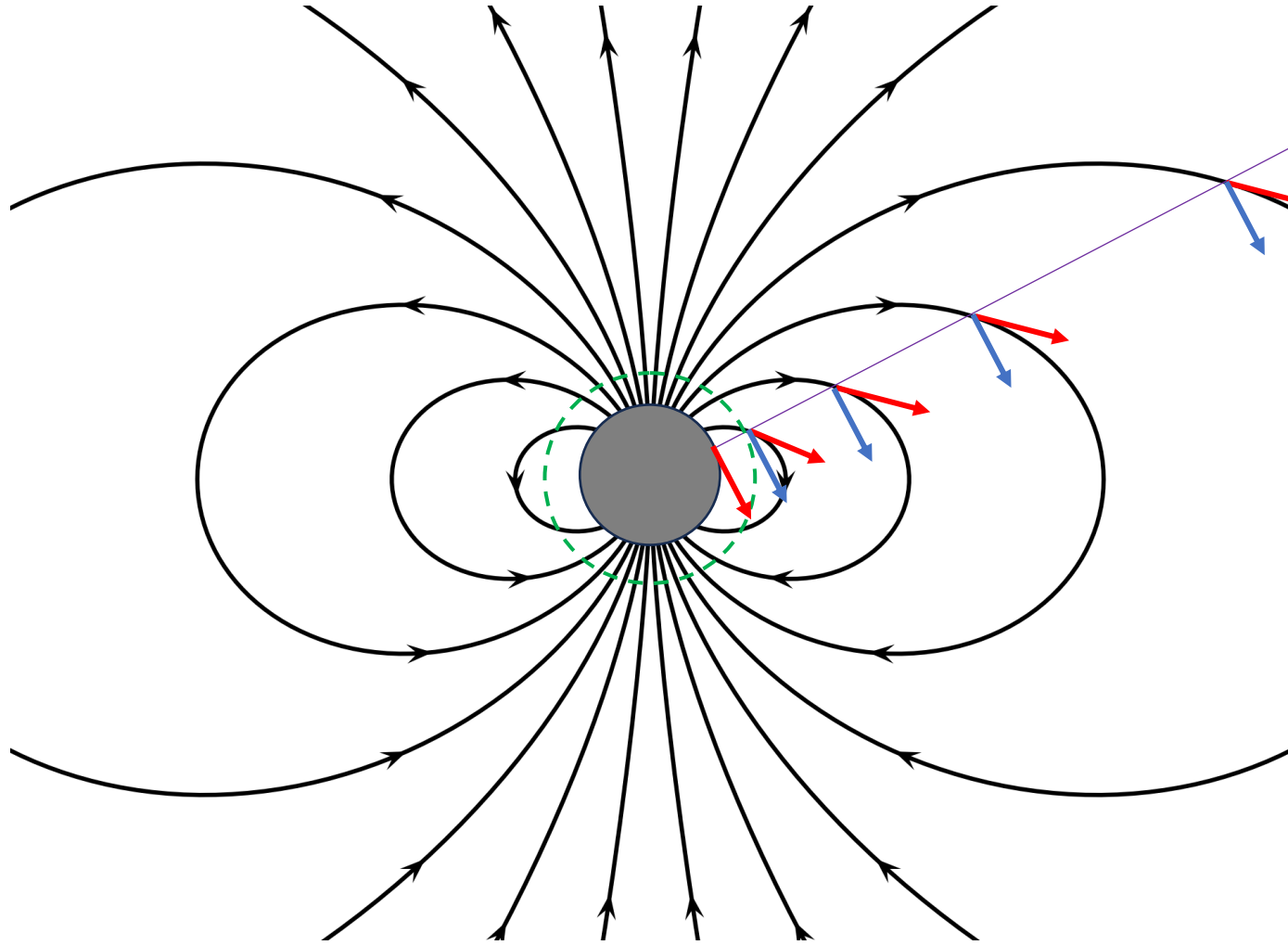
$$\frac{2}{k_0 \delta} \frac{dE_y}{dz} = i [PE_x + NE_y]$$

$\ell_E \gg \ell_B$: \mathbf{E} direction is frozen

$r_{pl} (\ell_E = \ell_B)$

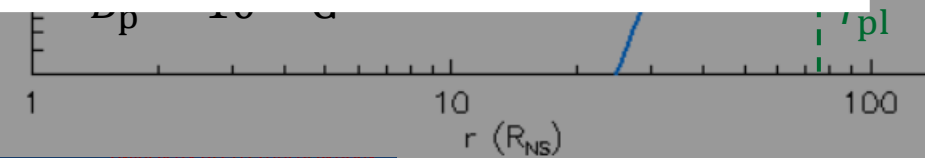
$\ell_E \ll \ell_B$: \mathbf{E} adapts to \mathbf{B}

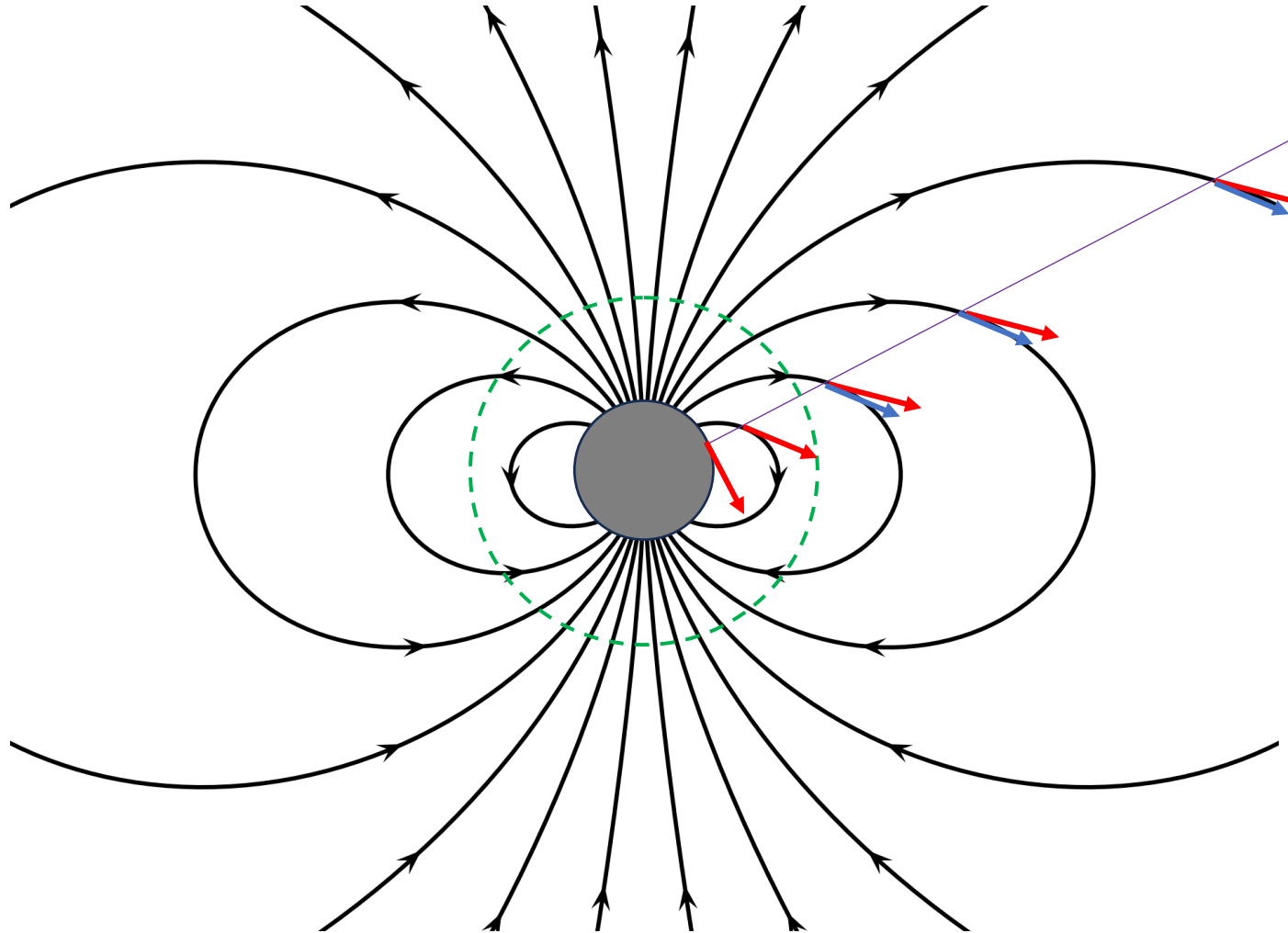




Small $r_{pl} \rightarrow$ large deviation

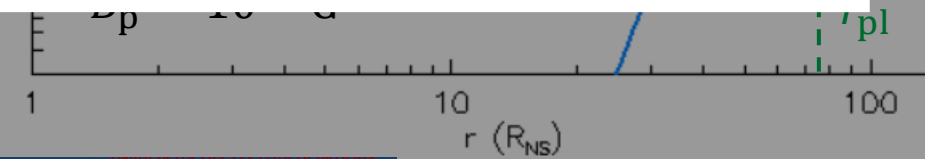
$l_E <$

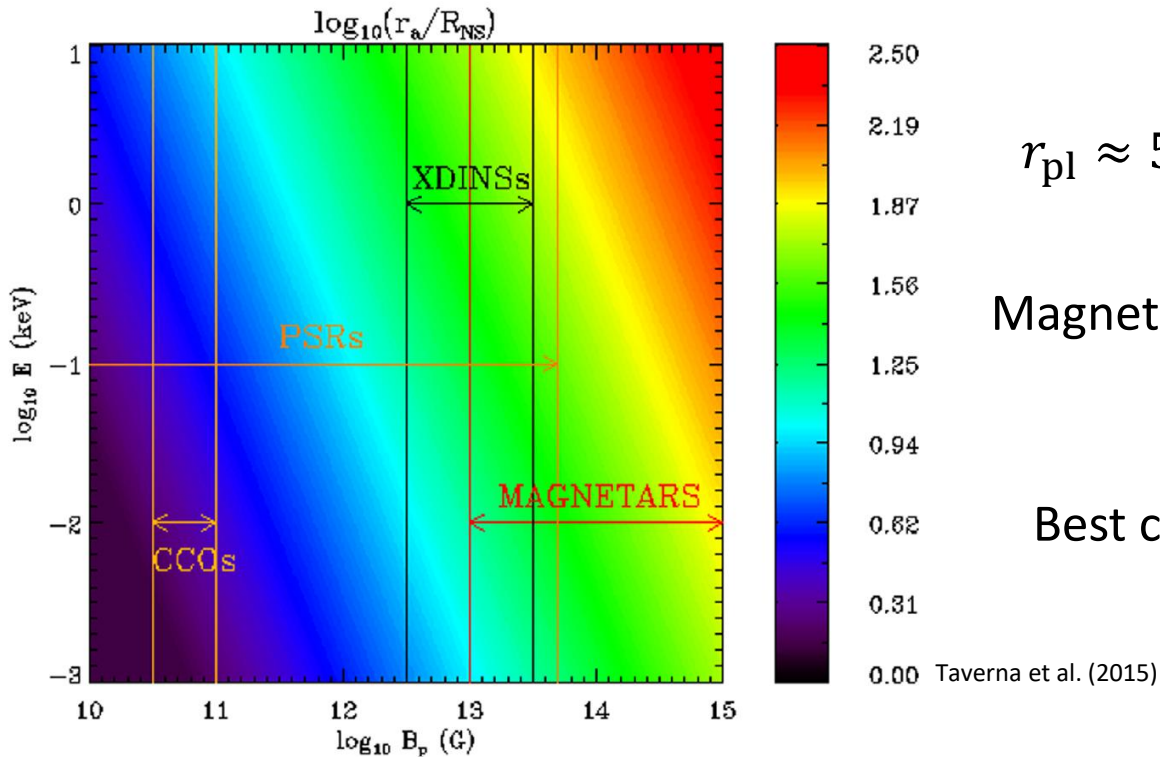




Large $r_{pl} \rightarrow$ small deviation

$l_E <$



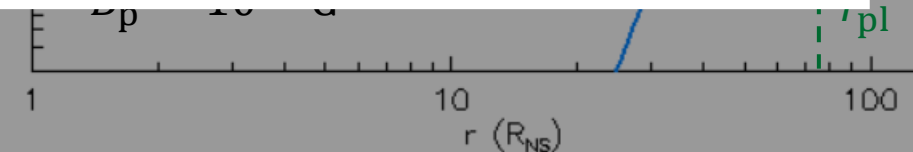


$$r_{pl} \approx 5 \left(\frac{B_{pol}}{10^{11} \text{ G}} \right)^{2/5} \left(\frac{\hbar\omega}{1 \text{ keV}} \right)^{1/5} \left(\frac{R_{NS}}{10 \text{ km}} \right)^{1/5} R_{NS}$$

Magnetars (with the strongest B) have the largest r_{pl}



Best candidates to observe polarization of surface emission (potentially very high)



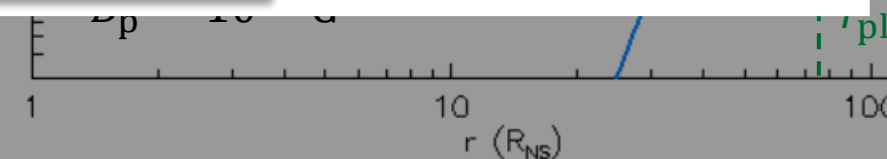
Test of vacuum birefringence depends as well on the size of the emitting region



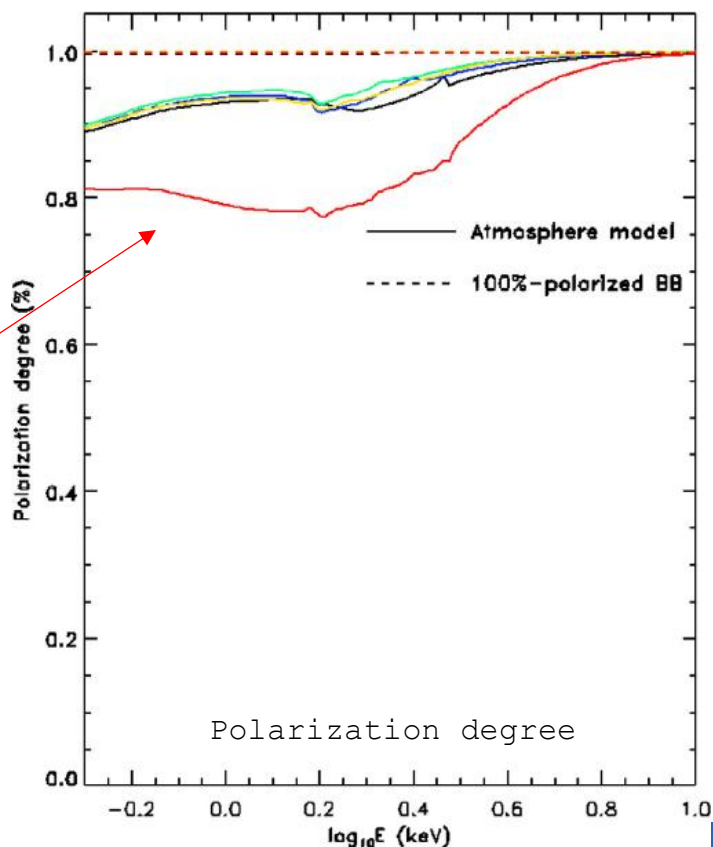
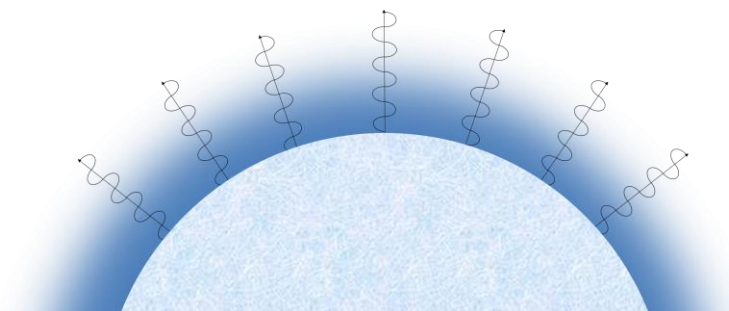
Small (polar) emitting region \Rightarrow
 Small depolarization
 (van Adelsberg & Perna 09)

Large emitting regions \Rightarrow
 Large depolarization
 (Taverna+ 20)

**Test of vacuum birefringence: high polarization
 from an extended region!**



- Surface photons reprocessed by a standard, magnetized atmosphere → high PD (X-mode)

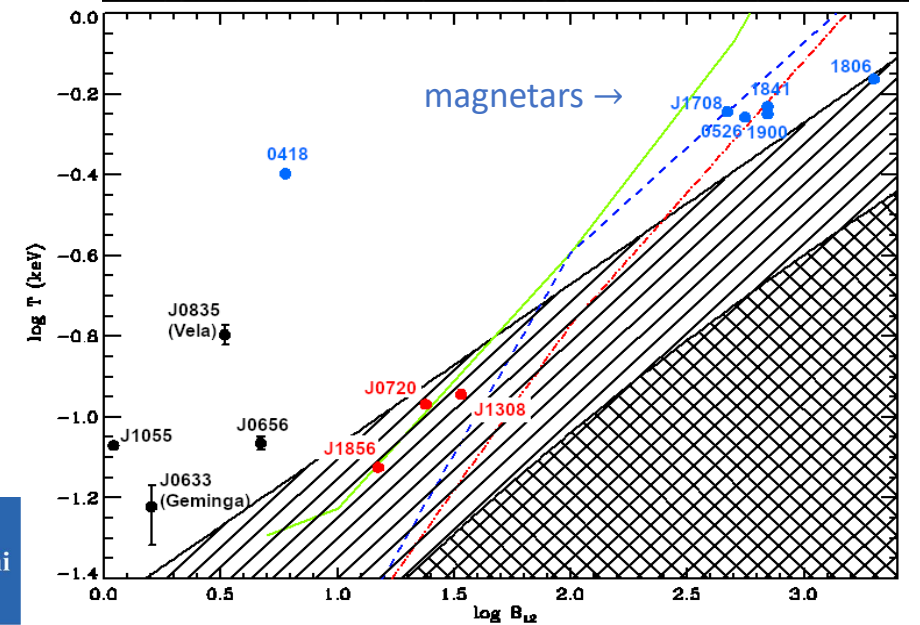
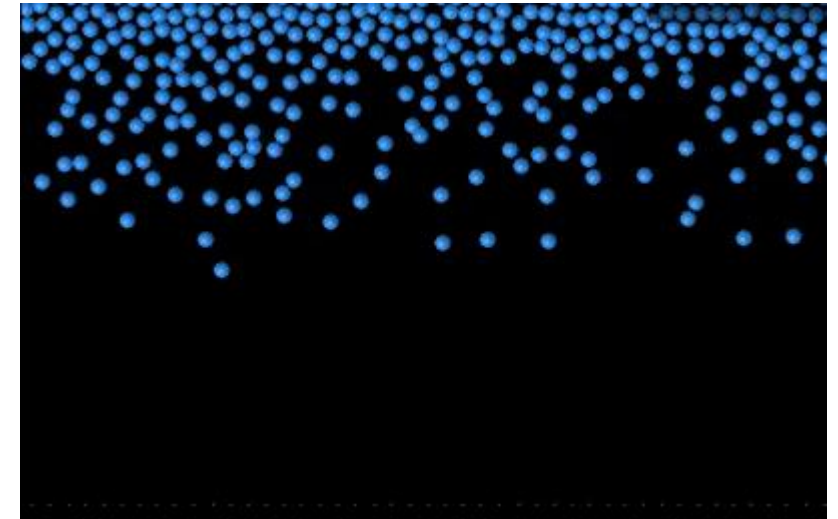


Taverna et al. (2020)

PD \gtrsim 80%

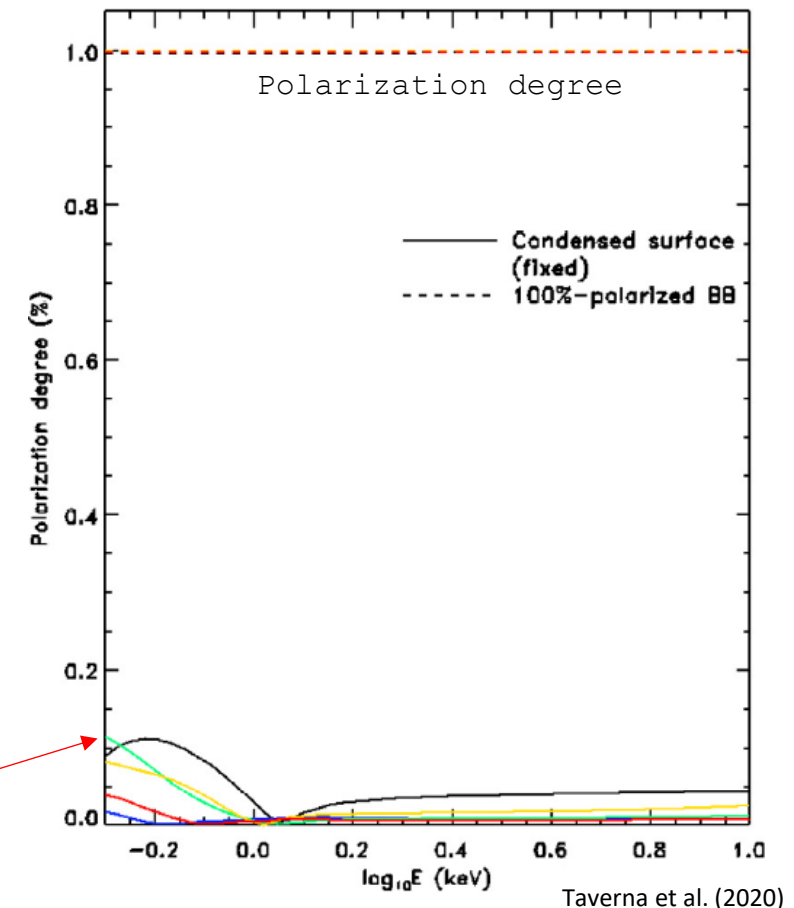
Surface emission models

- Surface photons reprocessed by a standard, magnetized atmosphere → high PD (X-mode)
- Very strong B -fields elongate atoms along the field direction → molecular chains are formed for sufficiently low T
- The atmosphere settles onto the surface and the (condensed) crust is left exposed

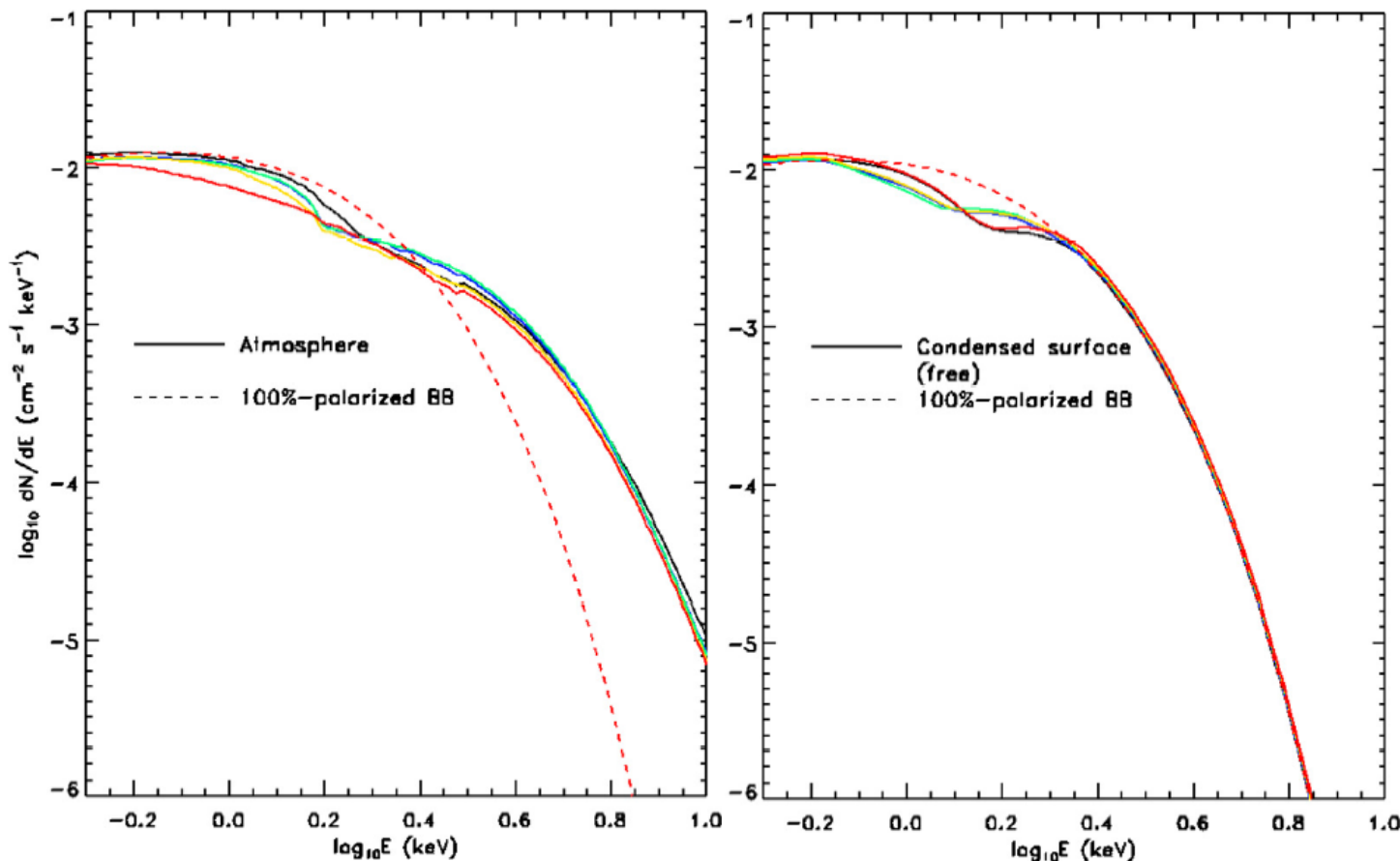


Taverna & Turolla (2024)

- Surface photons reprocessed by a standard, magnetized atmosphere → high PD (X-mode)
- Very strong B -fields elongate atoms along the field direction → molecular chains are formed for sufficiently low T
- The atmosphere settles onto the surface and the (condensed) crust is left exposed
- Much lower PD (both O- and X-)



PD \lesssim 20%



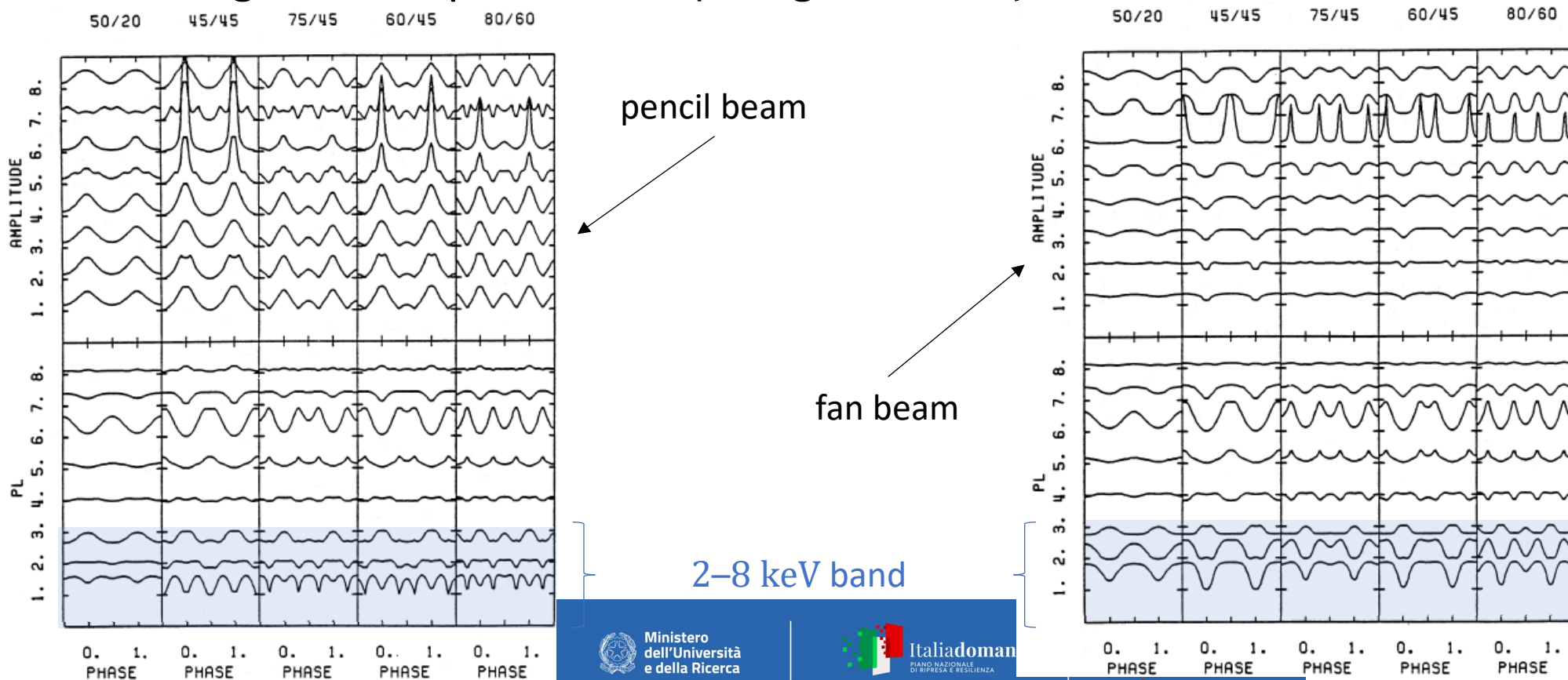
Spectra for atmosphere and condensed-surface model are similar (BB-like)

Polarization may help in disentangling the surface emission model

Taverna et al. (2020)

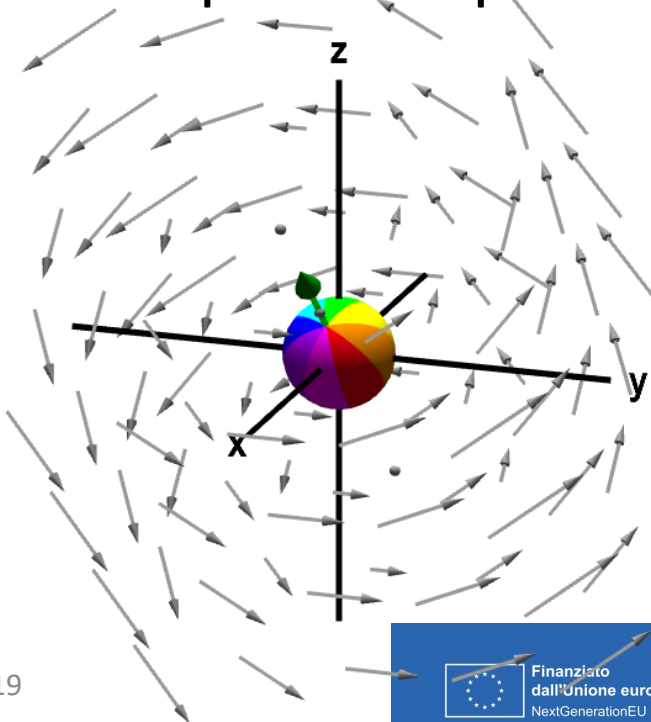
Theoretical expectations (XRPBs)

- Model for X-ray polarization in accreting X-ray pulsars (Meszaros et al. 1988)
 - radiation reprocessed by a plasma over the hot-spots (atmosphere or column)
 - Bremsstrahlung and Comptonization (in high B -fields)



Theoretical expectations (XRPCs)

- Model for X-ray polarization in accreting X-ray pulsars (Meszaros et al. 1988)
 - radiation reprocessed by a plasma over the hot-spots (atmosphere or column)
 - Bremsstrahlung and Comptonization (in high B -fields)
- Phase-dependent polarization angle \rightarrow Rotating Vector Model (RVM)

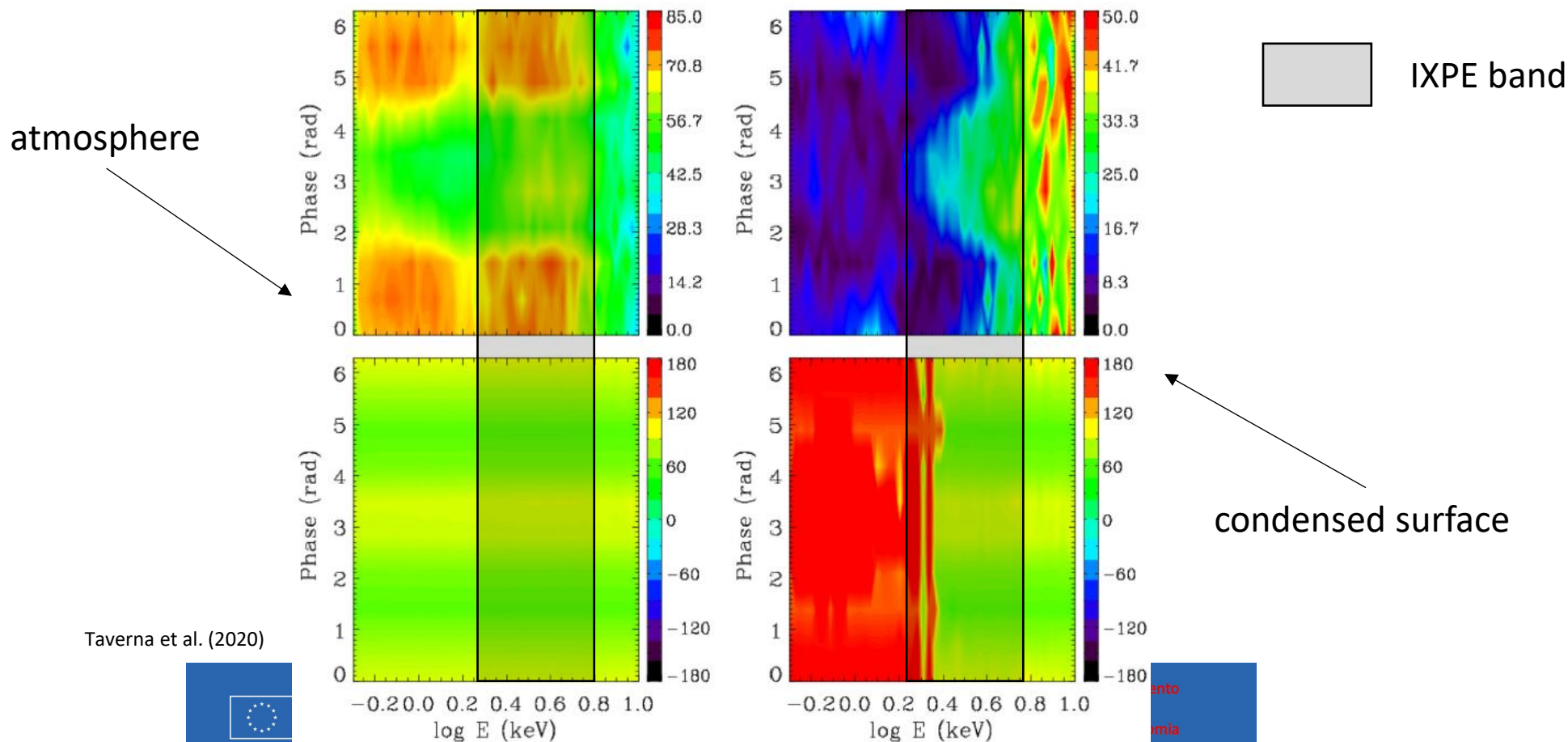


$$\tan(\text{PA}) = \frac{\sin \xi \sin \phi}{\cos \chi \sin \xi \cos \phi - \sin \chi \cos \xi}$$

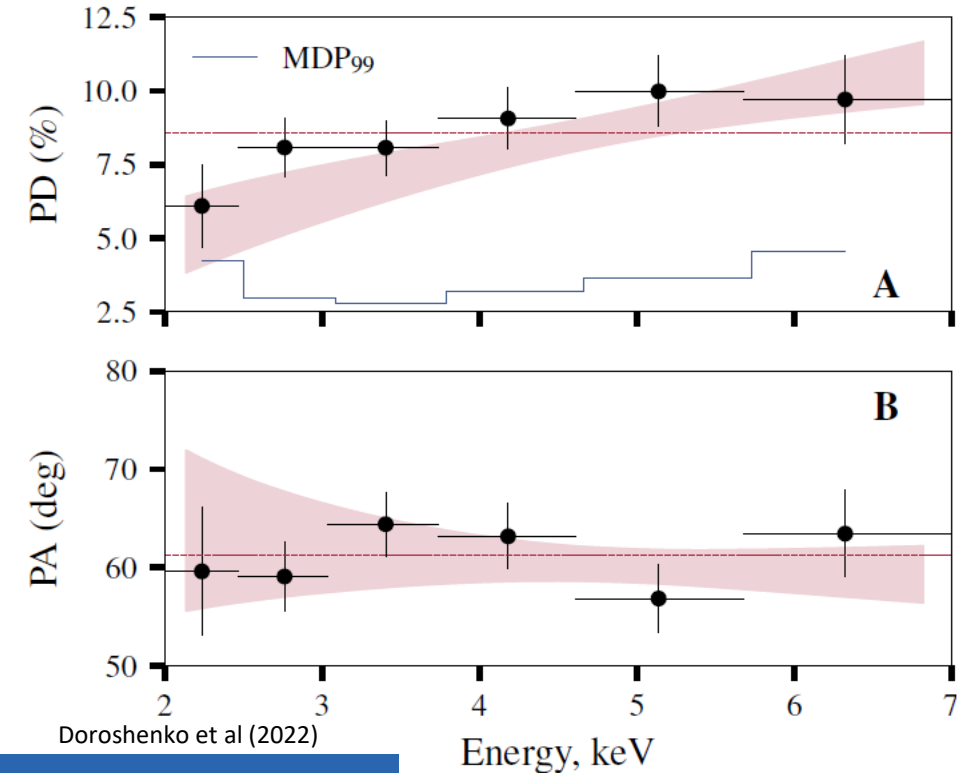
- dipolar magnetic field topology
- small emitting regions (hot-spots)

Theoretical expectations (magnetars)

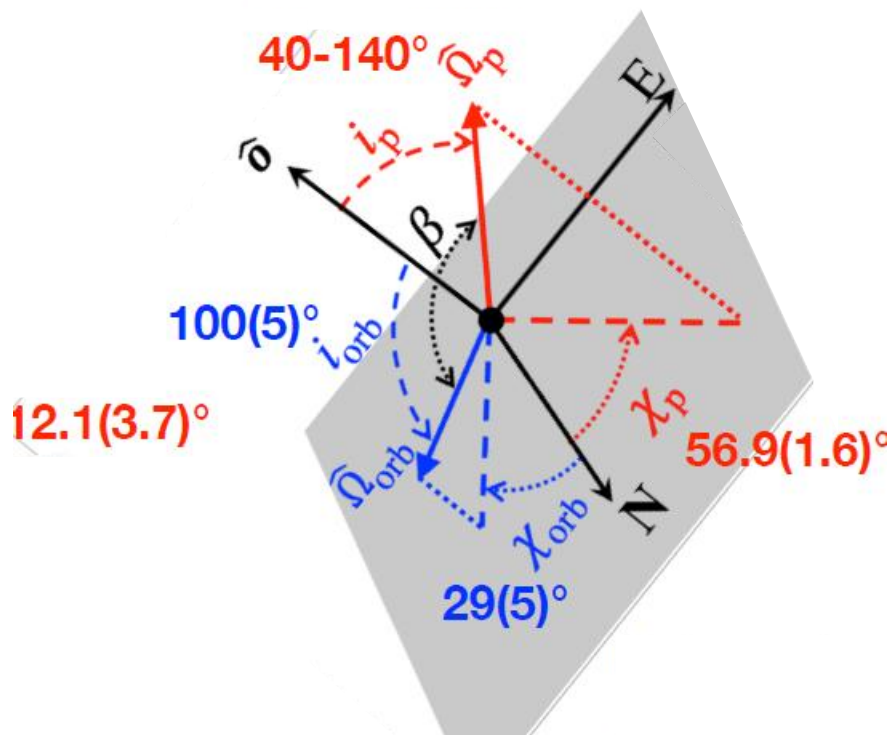
- Emission coming from the whole star surface (covered by an atmosphere or with condensed surface exposed)



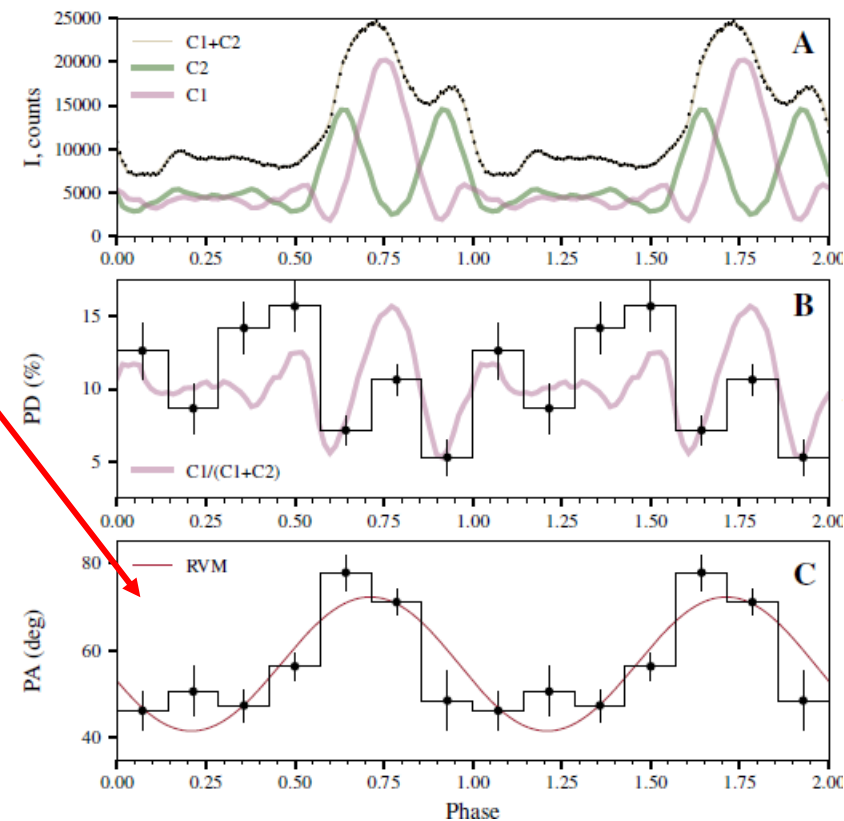
- Strongly magnetized NS ($B = 4.5 \times 10^{12}$ G) – intermediate-mass binary
- Two observations
 - February, 17–24 2022 (Doroshenko et al. 2022)
 - January 18–21, February 3–5 2023 (Heyl et al. 2023)
- Polarization detected:
 - $PD = 8.6\%$ – $PA \approx 60^\circ$ E (17σ)
- Well below the expectations (60–80%, Meszaros+88, Caiazzo & Heyl 21)



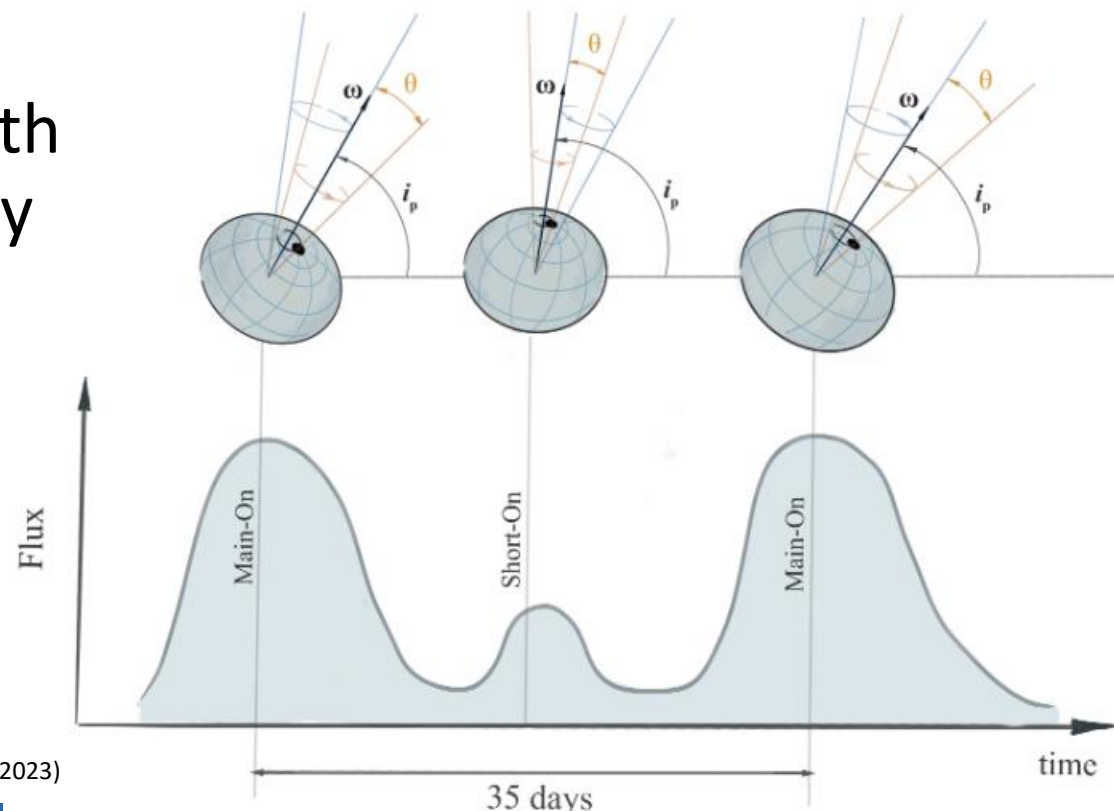
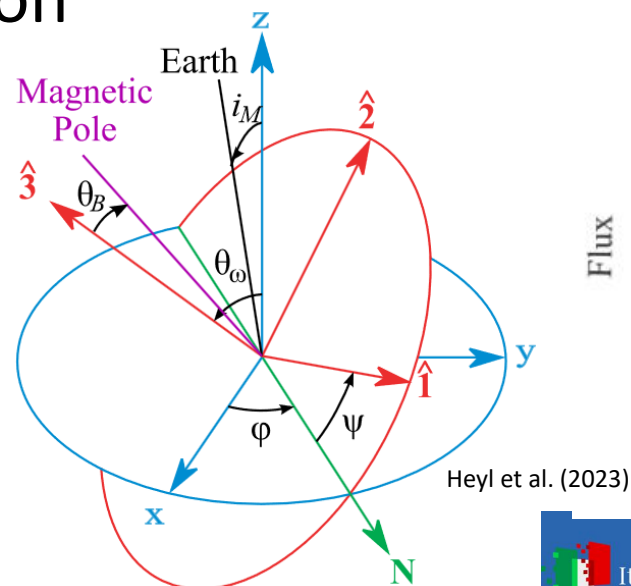
- RVM fit of the phase-dependent PA helped in constraining spin and magnetic axis inclinations for the first time for an XRP



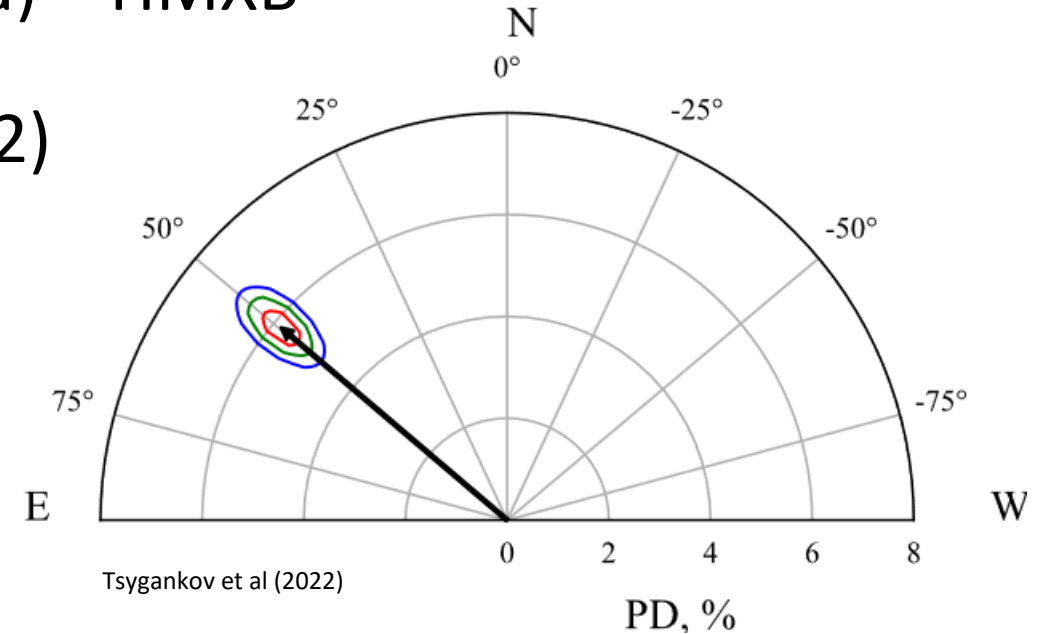
Doroshenko et al (2022)



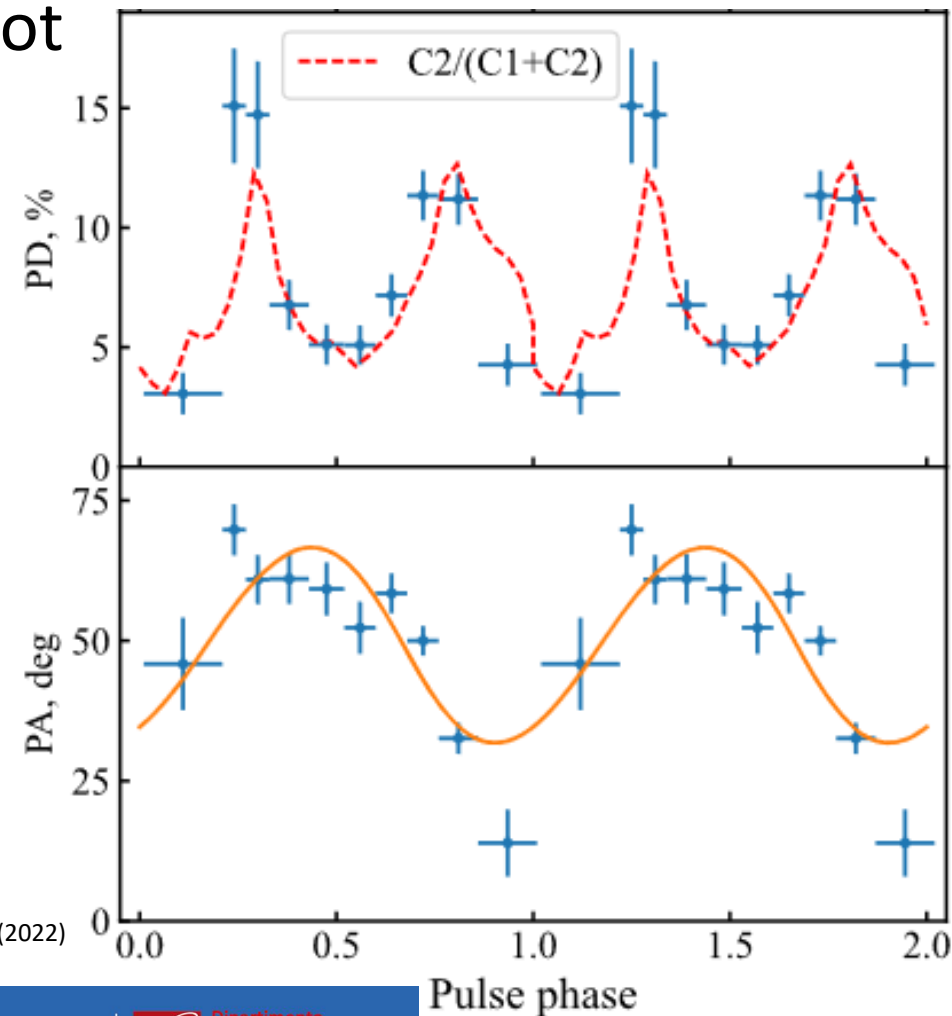
- RVM fit of the phase-dependent PA helped in constraining spin and magnetic axis inclinations for the first time for an XRP
- Second, time-dependent observation (with PA changing by $\approx 10^\circ$) allowed for a study of the source precession



- Strongly magnetized NS ($B = 3\text{--}4 \times 10^{12}$ G) – HMXB
- Observed in two slots (Tsygankov et al. 2022)
 - January, 29–31 2022 (low state)
 - July, 4–7 2022 (high state)
- Polarization detected:
 - Low state: Not significant
 - High state: PD = 5.6% – PA = 47° E (15σ)
- Still below the expectations (60–80%, Meszaros+88) – to be understood

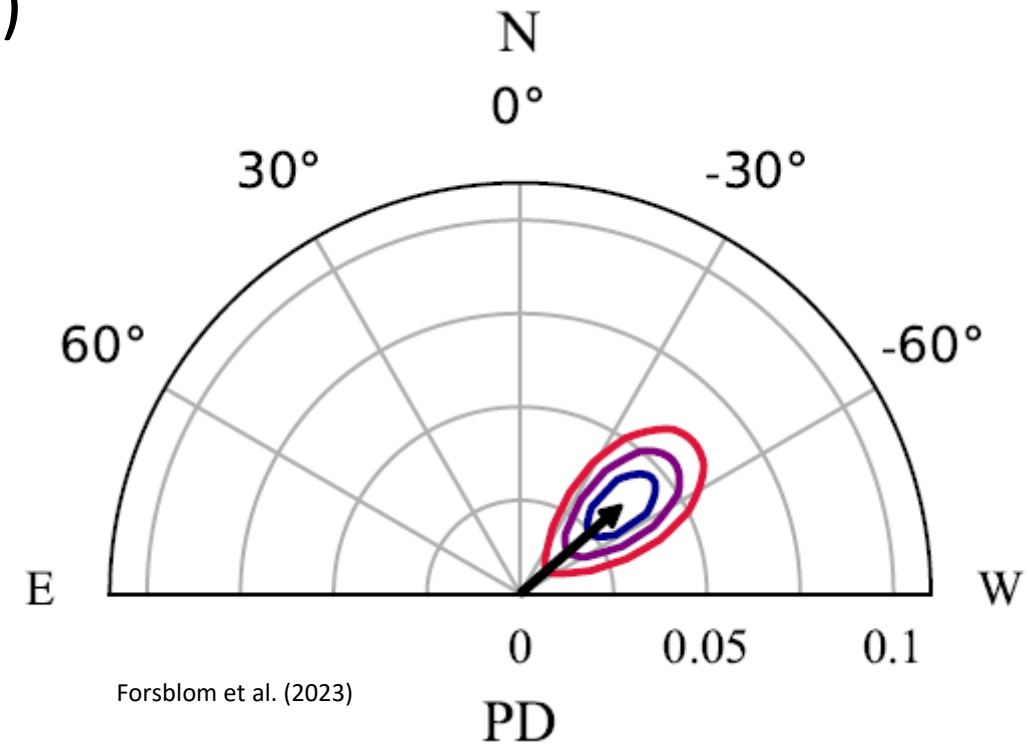


- Phase-dependent PD well explained by a 2-spot model, slightly displaced from antipodal position (Kraus+ 96)
- PA still follows a sinusoidal behavior (RVM)
- Constraints on the spin/magnetic axis inclinations: $\chi \approx 70^\circ - \xi \approx 20^\circ$

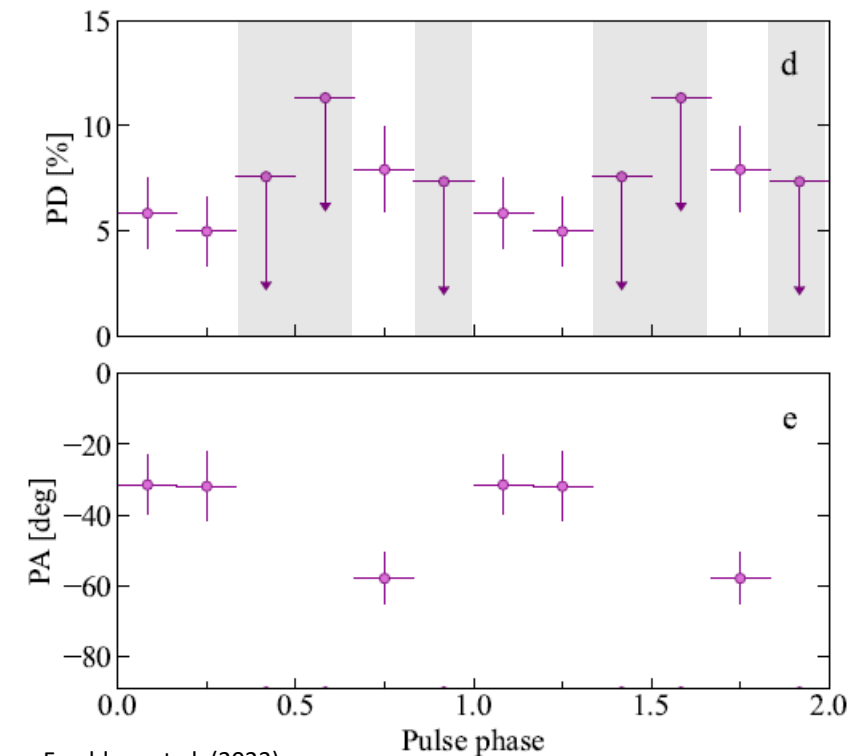


Tsygankov et al (2022)

- HMXB – Highly magnetized ($B \approx 3 \times 10^{12}$ G)
- Observation (Forsblom et al. 2023):
 - April, 15–21 2022 (low state)
- Measurement: PD = 3.9% ($\text{MDP}_{99} = 2.6\%$)
PA = 52° W



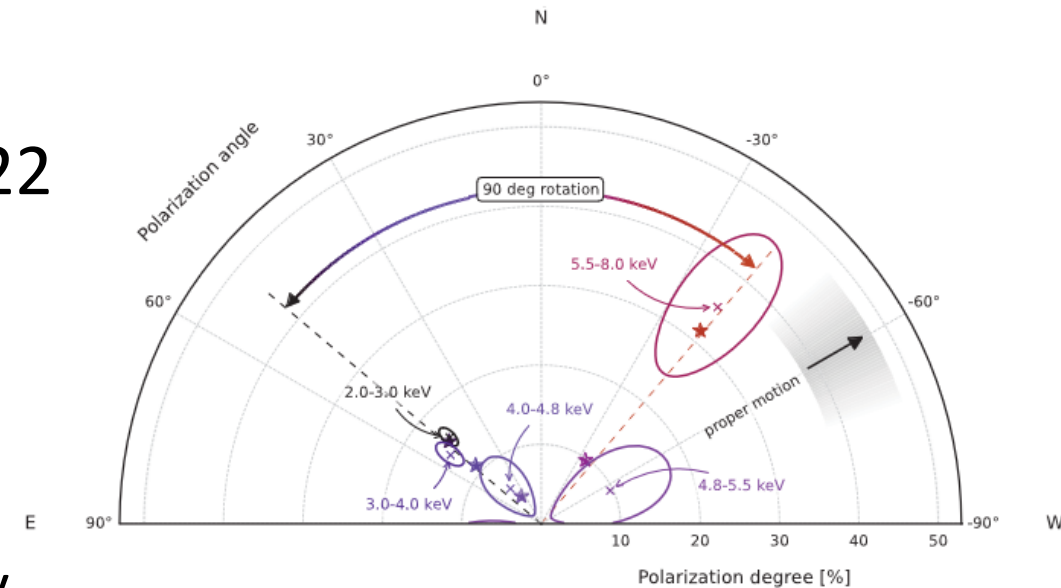
- Phase-dependent PD only marginally above the MDP_{99}
- Correspondent PA is not significantly determined (but RVM oscillations seem to be plausible)



Forsblom et al. (2023)

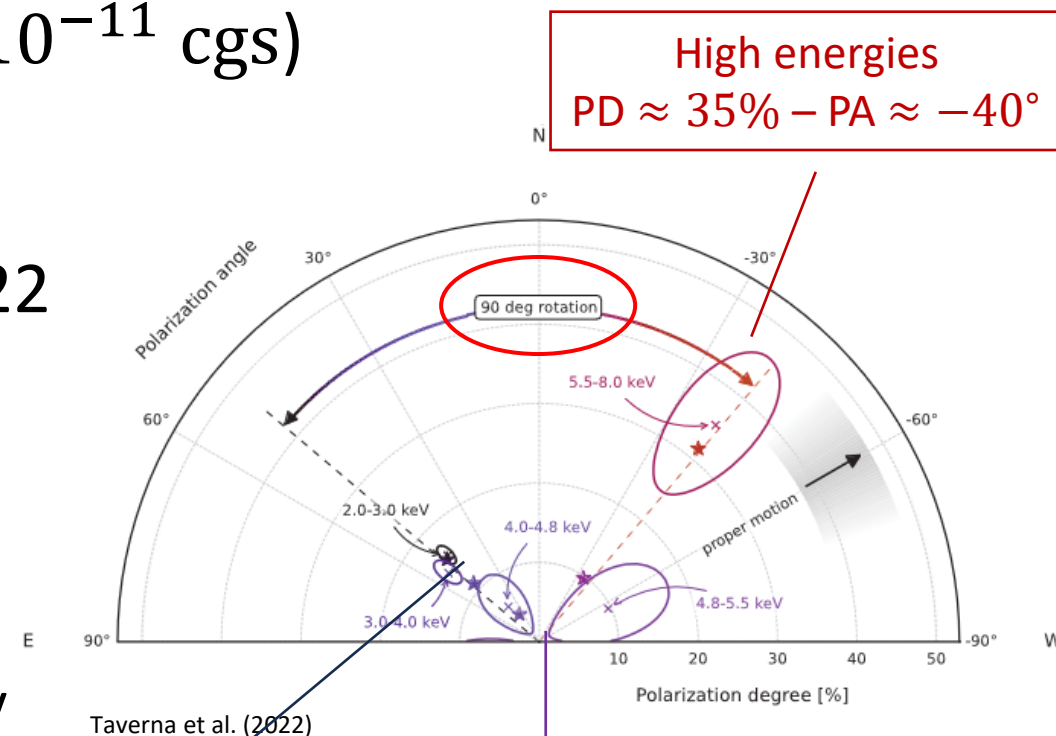
- In all the observed accreting XRPs, PD is much lower than expected (despite the strong magnetic field points to high PD and X-mode photons)
- New models are required
 - The atmosphere above the surface is not a «standard», cooling atmosphere (heating from the accretion flow)
 - Partial mode conversion at the vacuum resonance (inside the IXPE energy band) may determine a depolarization of the emitted radiation

- Brightest among magnetars ($F_{2-10}^{\text{unabs}} \approx 7 \times 10^{-11}$ cgs)
- $B_{p\dot{p}} \approx 1.5 \times 10^{14}$ G
- Observed once January 31–February 27, 2022
- Spectrum BB+PL
- Polarization measurement (2–8 keV):
 - PD = 13.5% (17σ) – PA $\approx 50^\circ$ E
 - PD and PA change with energy in a non-trivial way



Taverna et al. (2022)

- Brightest among magnetars ($F_{2-10}^{\text{unabs}} \approx 7 \times 10^{-11}$ cgs)
- $B_{p\dot{p}} \approx 1.5 \times 10^{14}$ G
- Observed once January 31–February 27, 2022
- Spectrum BB+PL
- Polarization measurement (2–8 keV):
 - PD = 13.5% (17σ) – PA $\approx 50^\circ$ E
 - PD and PA change with energy in a non-trivial way

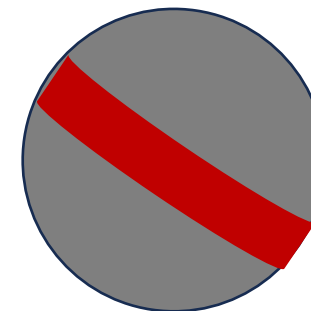


High energies
 PD $\approx 35\%$ – PA $\approx -40^\circ$

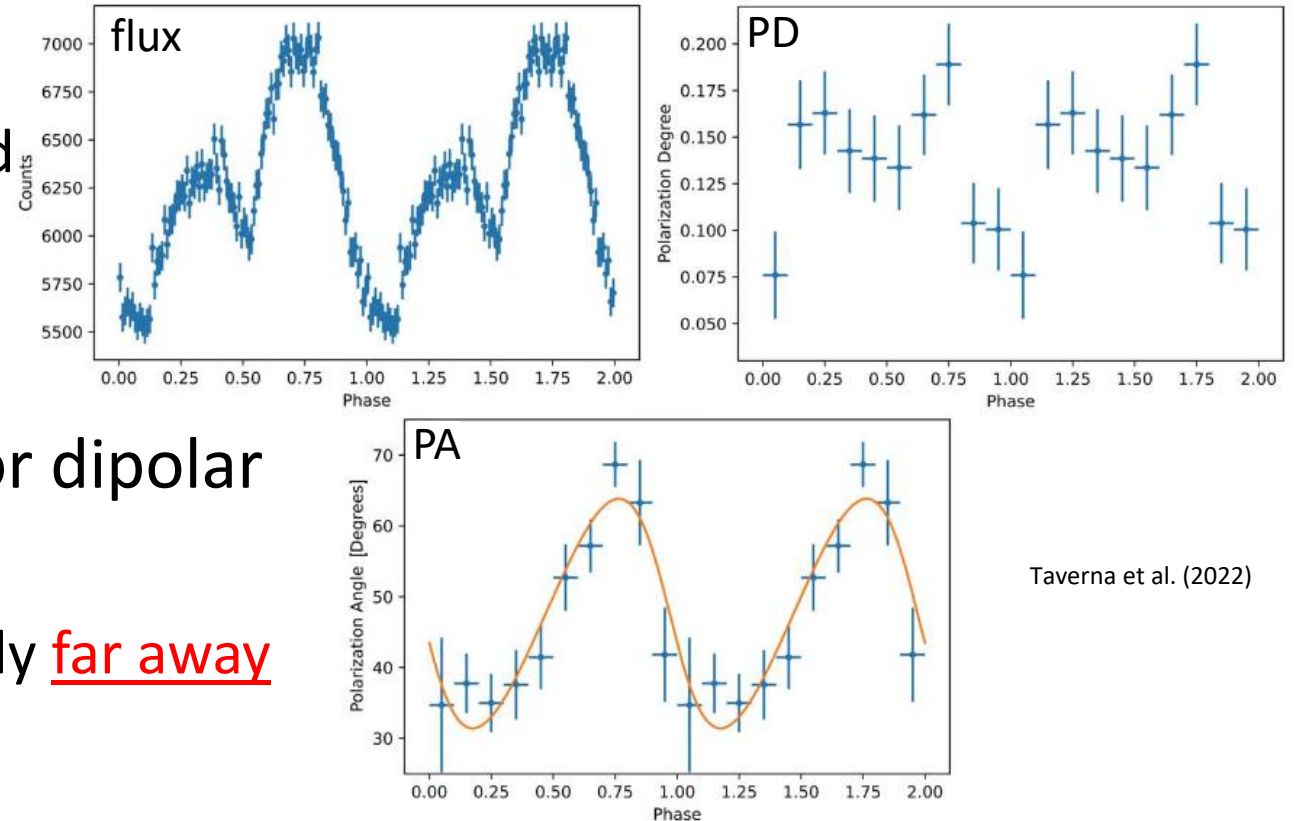
Low energies
 PD $\approx 15\%$ – PA $\approx 50^\circ$

4–5 keV
 PD ≈ 0

- Results are compatible with the magnetar model
 - 90°-swing → X- and O-modes (ultra-strong B -fields $\gtrsim 10^{13}$ G independently from $P-\dot{P}$)
 - PD at high energies ($\approx 35\%$) → PL tail populated by RCS photons
 - According to the model RCS photons are X-mode → O-mode at low energies
 - Low PD + O-mode photons → **condensed surface exposed** (equatorial-belt emission geometry)

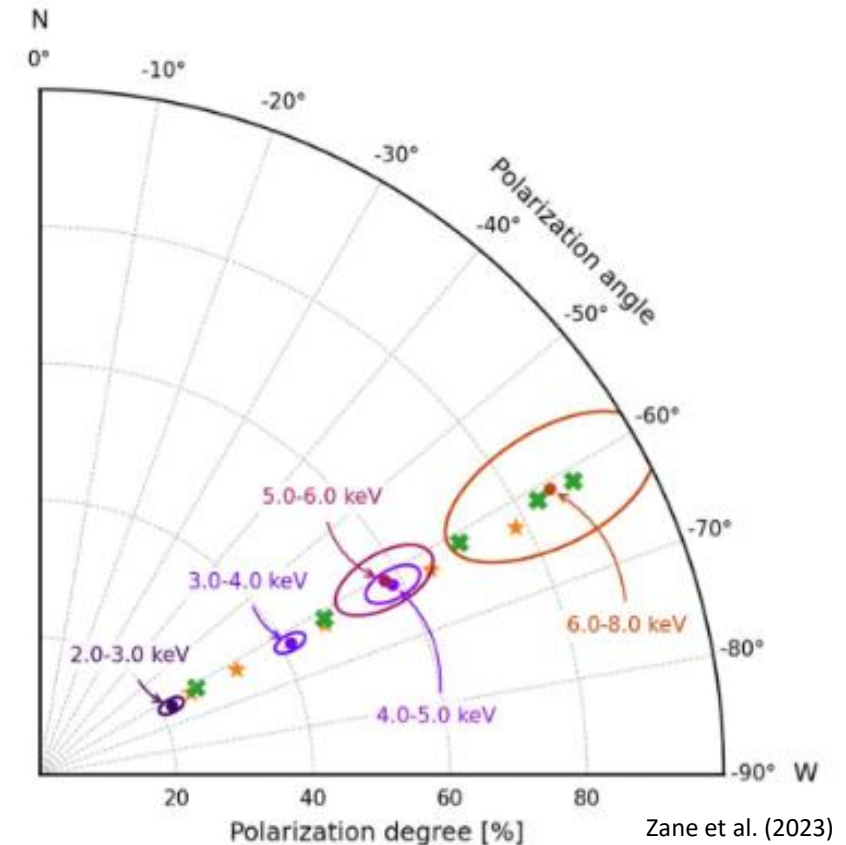


- Phase dependent results
 - PD is in-phase with the LC (determined at the surface)
 - PA is sinusoidal (RVM)
- RVM for extended regions holds for dipolar fields only
 - In the magnetar model B is dipolar only far away from the surface
- Effect explained if vacuum birefringence is at work!



Taverna et al. (2022)

- 2nd brightest magnetar ($F_{2-10}^{\text{unabs}} \approx 3 \times 10^{-11}$ cgs)
- $B_{P\dot{P}} \approx 5 \times 10^{14}$ G
- Observed once September 19–October 8, 2022
- Spectrum BB+PL or BB+BB?
- Polarization measurement (2–8 keV):
 - PD = 35% (22.5σ) – PA $\approx 60^\circ$ W
 - Polarization direction is constant within the IXPE band
 - PD at 6–8 keV: $\approx 85\%$ (MDP₉₉ = 50%)
the highest measured so far!

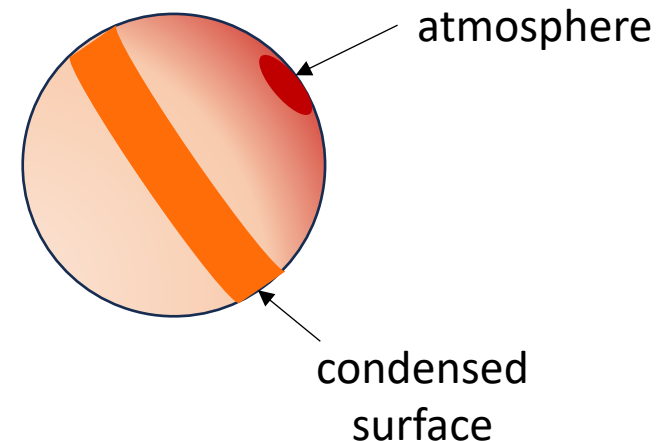


- Theoretical interpretation

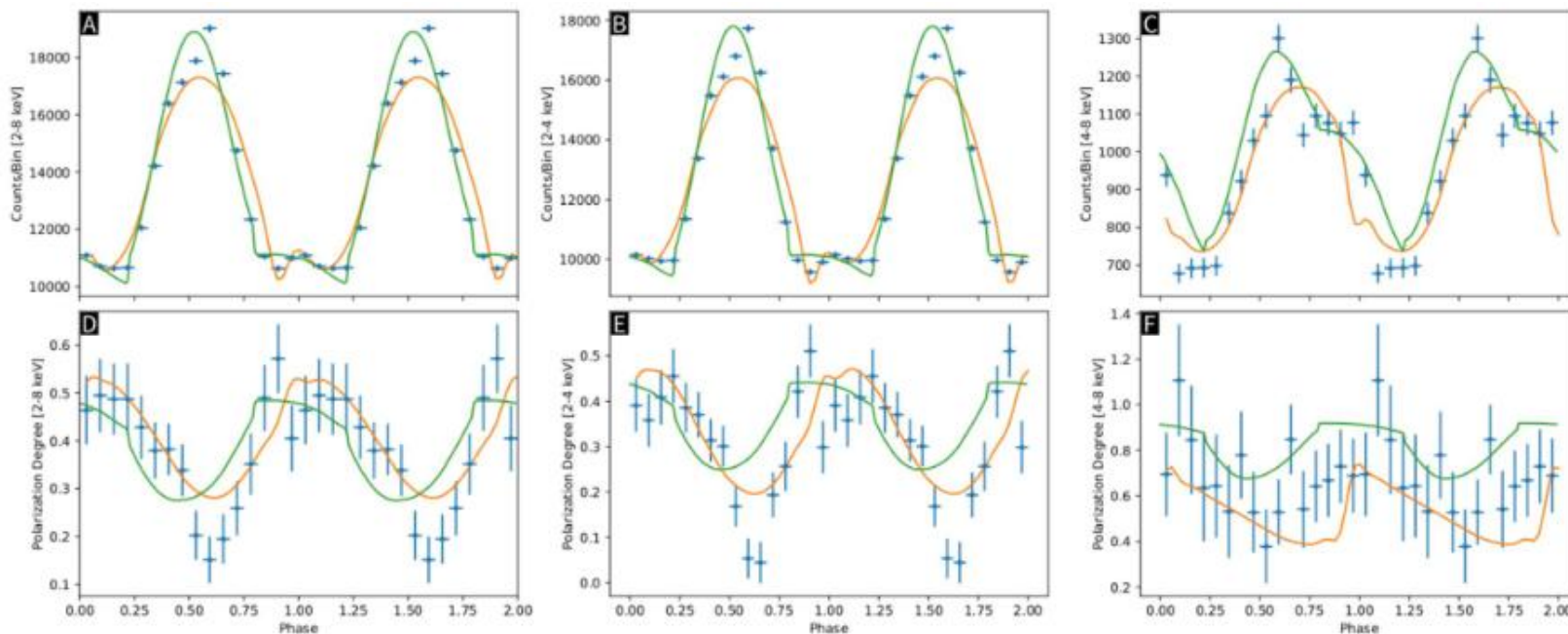
- high PD points towards plasma reprocessing → NS atmosphere
- PD at high energies too large for RCS ($\approx 33\%$) → BB+BB (2 distinct thermal regions)
- PD at low energies too small for atmosphere → condensed surface



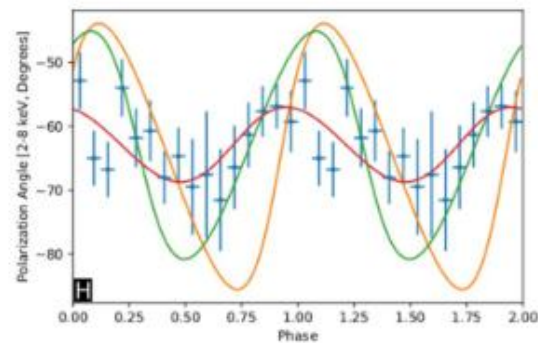
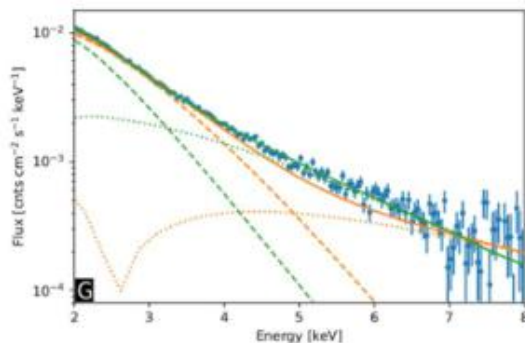
Phase transition across the surface



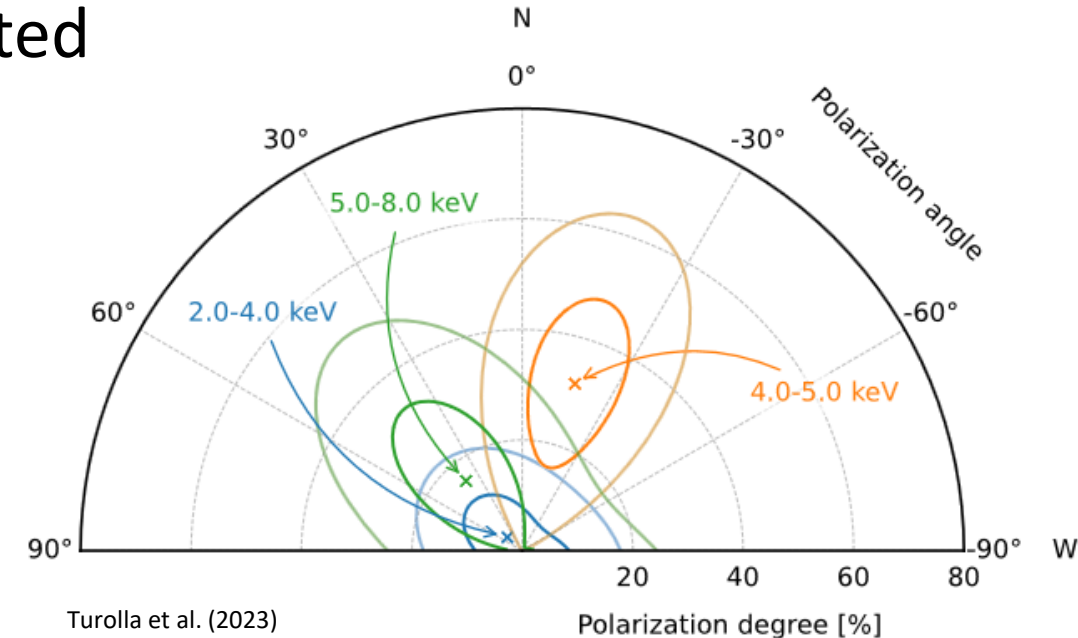
- Phase-dependent results are coherently explained by the model



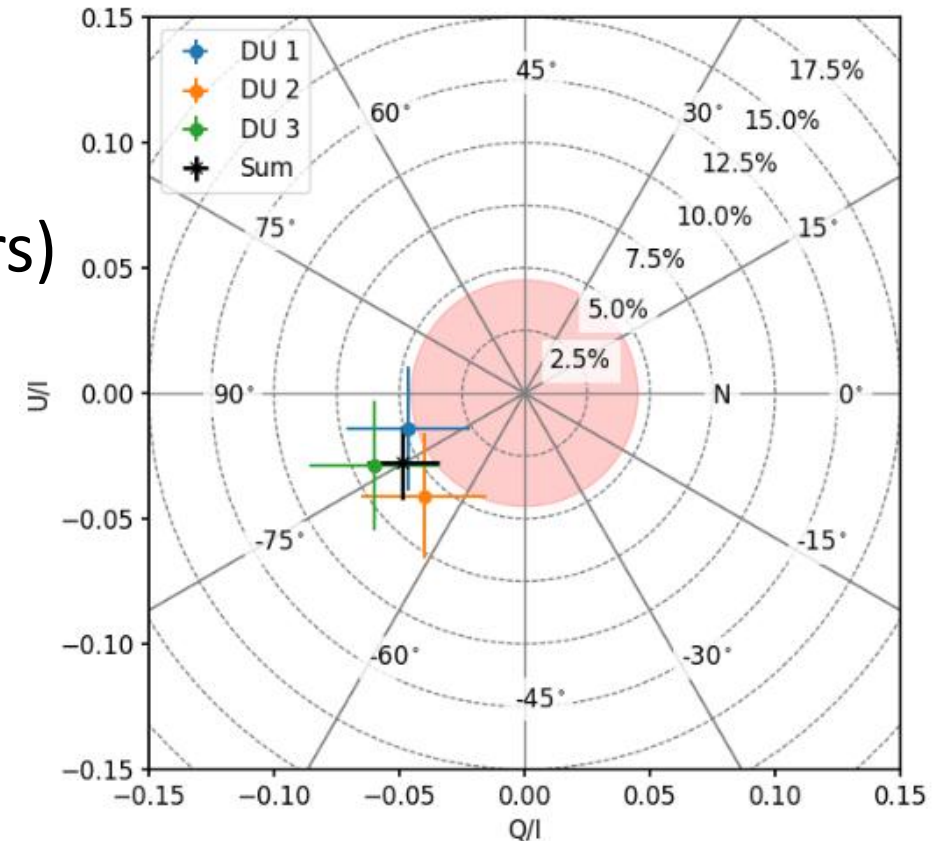
Spectral decomposition (atmo+CS)



- Emitted the strongest giant flare ever detected (December 27, 2004)
- $B_{P\dot{P}} \approx 8 \times 10^{14}$ G (strongest B -field)
- Observed once March 22–April 13, 2023 (+ XMM contemporary campaign)
- Marginally significant IXPE measurement
 - Unexpectedly low flux (4×10^{-12} cgs, $\approx 1/10$ historical)
 - Occurrence of solar flares during observation
 - PD $\approx 32\%$ (4–5 keV, 99% c.l.)

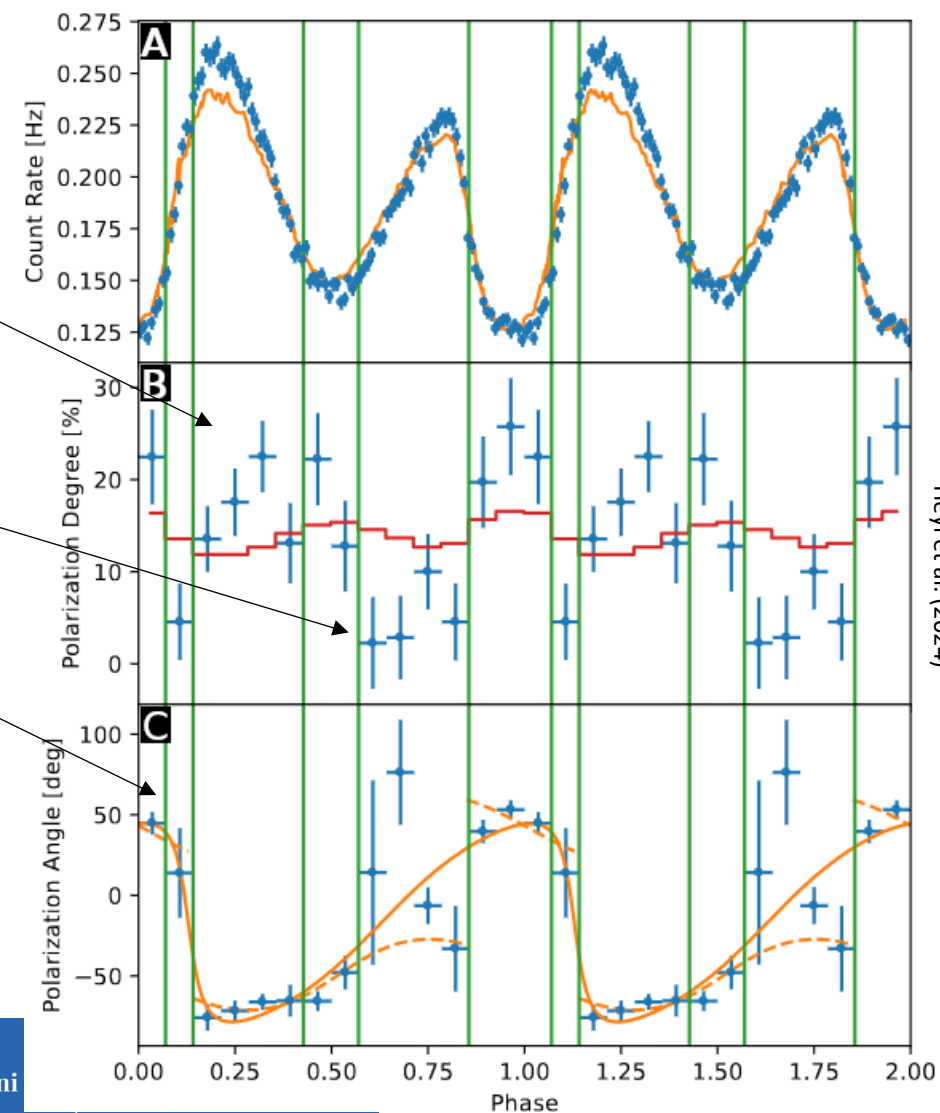


- Observed once, June 2–July 6, 2023 + XMM & NICER observations
- $B_{p\dot{p}} \approx 6 \times 10^{13}$ G (among low-field magnetars)
- Averaged (2–8 keV) PD = 5.6%, only significant at low energies
- Spectral fit BB+PL is not good enough → adding an absorption line the fit improves
- Previous studies (Pizzocaro+ 19) invoked the presence of a magnetic loop where proton cyclotron scattering occurs (then $B \approx 10^{14}$ G)

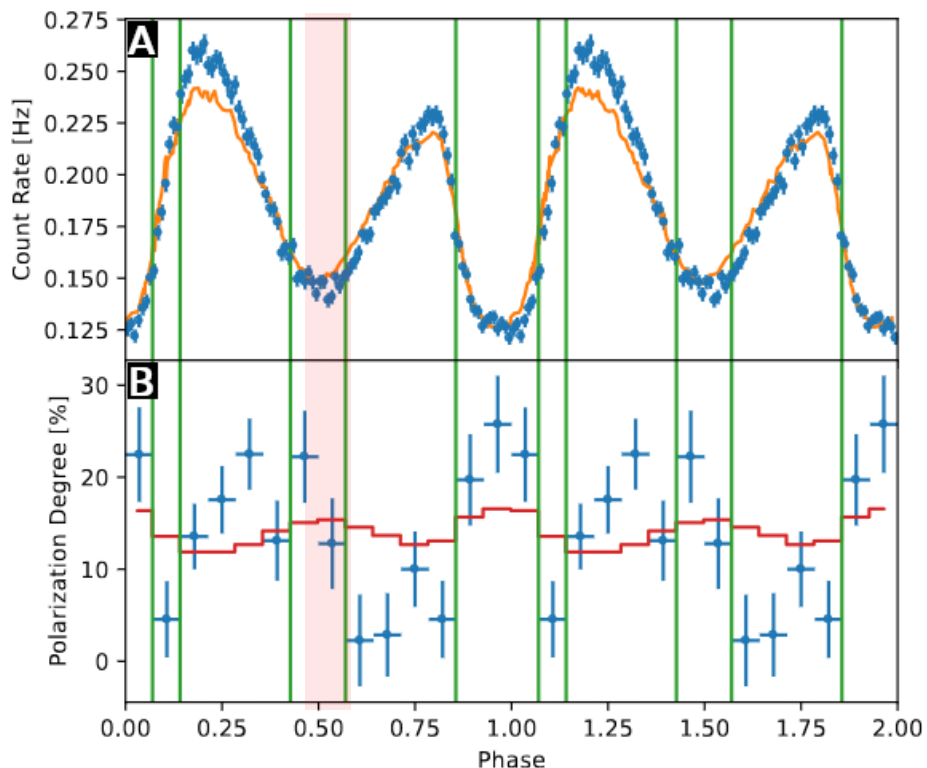


Heyl et al. (2024)

- Peculiar phase-dependent behavior
 - Polarization up to $\approx 25\%$ (well above MDP_{99}) at particular phases (corresponding to the rise and maximum of the primary LC peak)
 - Secondary peak basically unpolarized
 - PA well fitted by a RVM in which photons are assumed to change mode (from O- to X- and vice versa)

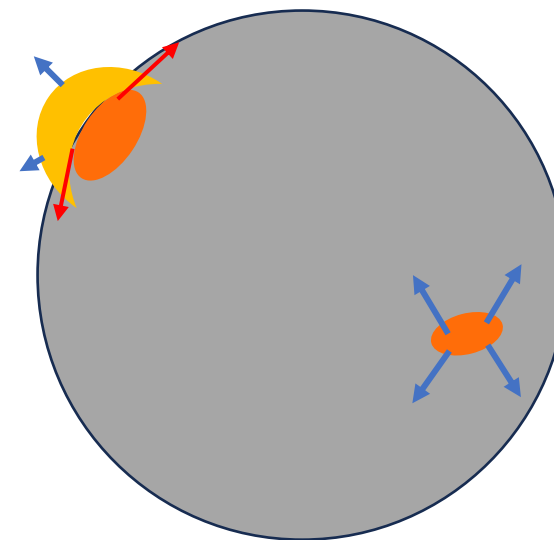


- Theoretical interpretation (in terms of the magnetic-loop model)

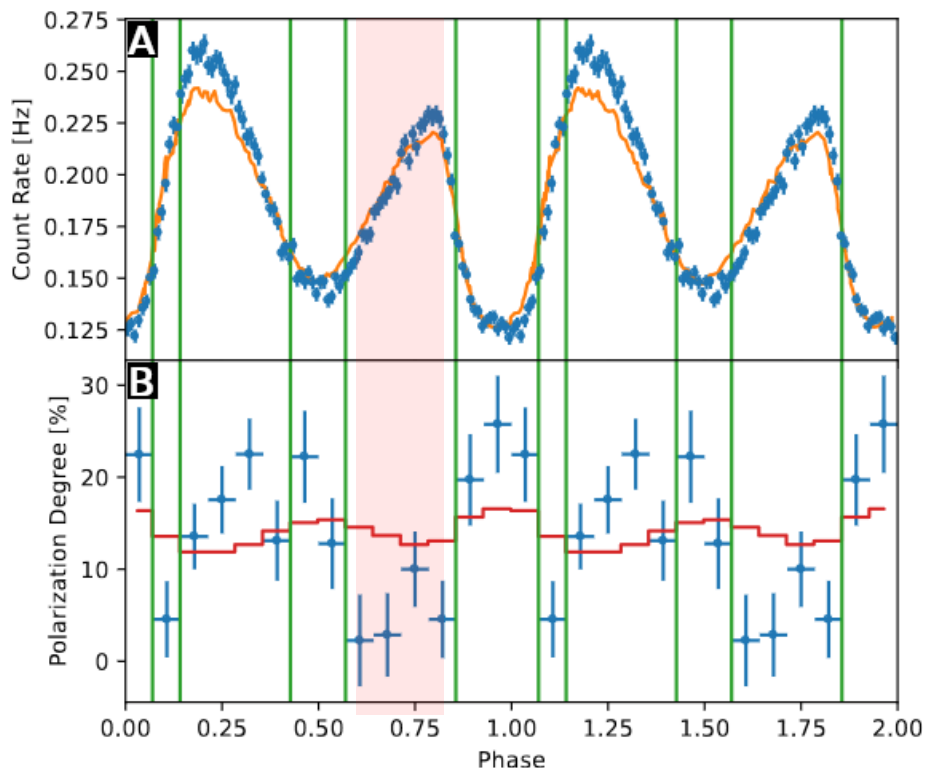


2 condensed-surface hotspots are present on the NS surface

The protons magnetic loop scatters away X-mode photons

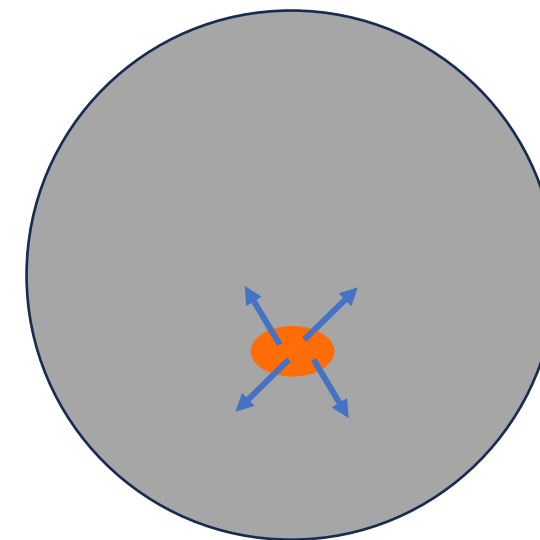


- Theoretical interpretation (in terms of the magnetic-loop model)

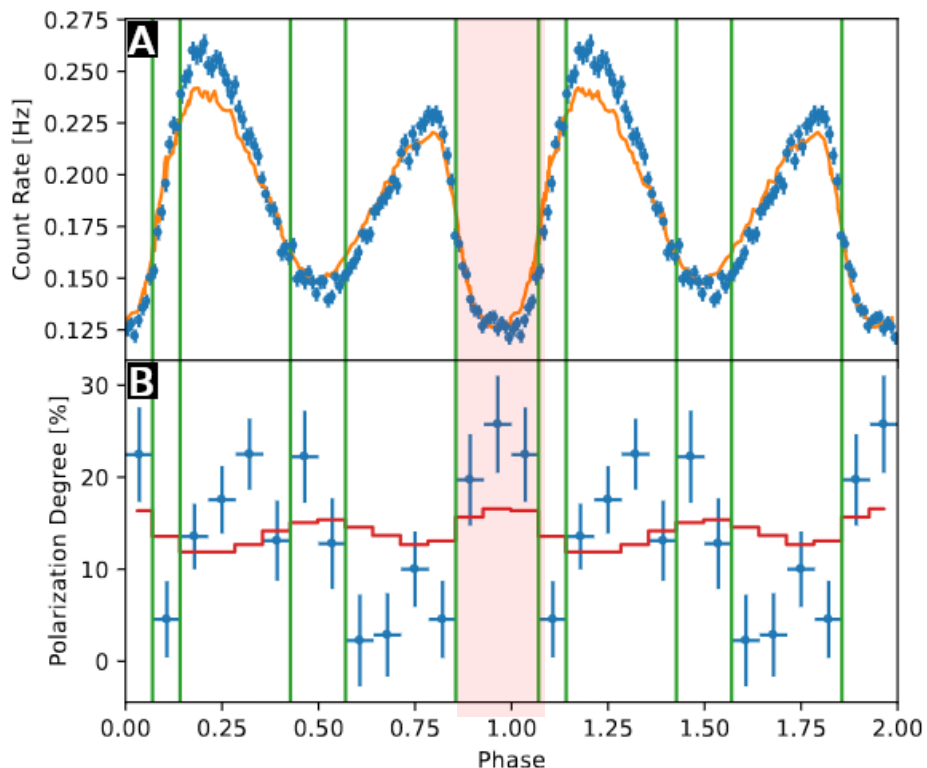


2 condensed-surface hotspots are present on the NS surface

The protons magnetic loop scatters away X-mode photons

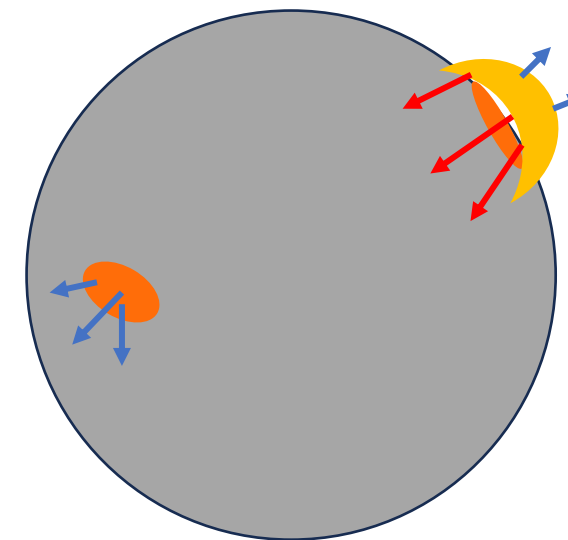


- Theoretical interpretation (in terms of the magnetic-loop model)

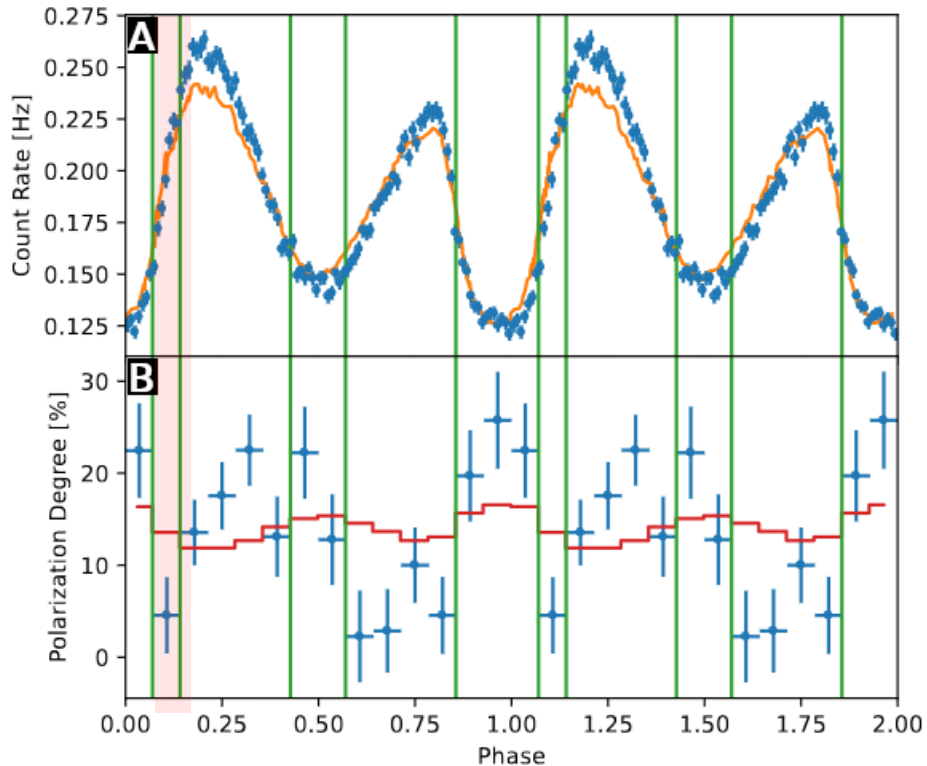


2 condensed-surface hotspots are present on the NS surface

The protons magnetic loop scatters away X-mode photons

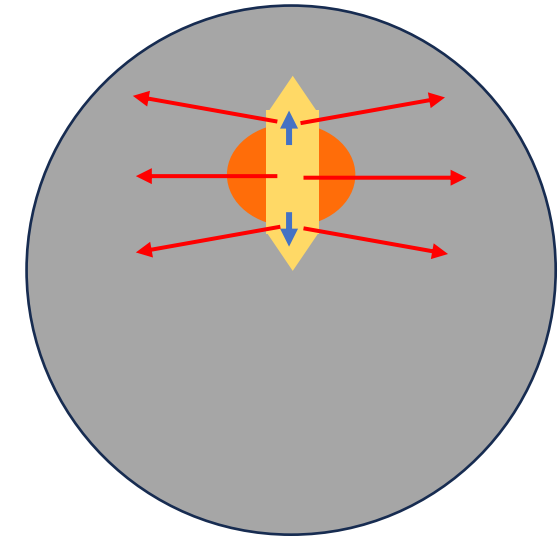


- Theoretical interpretation (in terms of the magnetic-loop model)

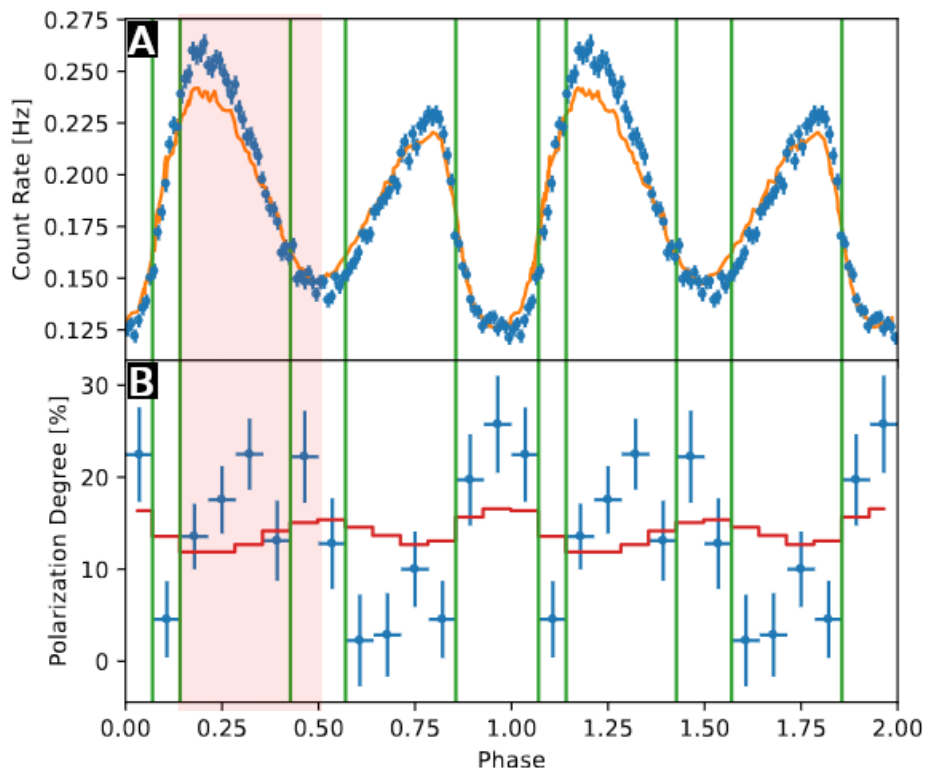


2 condensed-surface hotspots are present on the NS surface

The protons magnetic loop scatters away X-mode photons

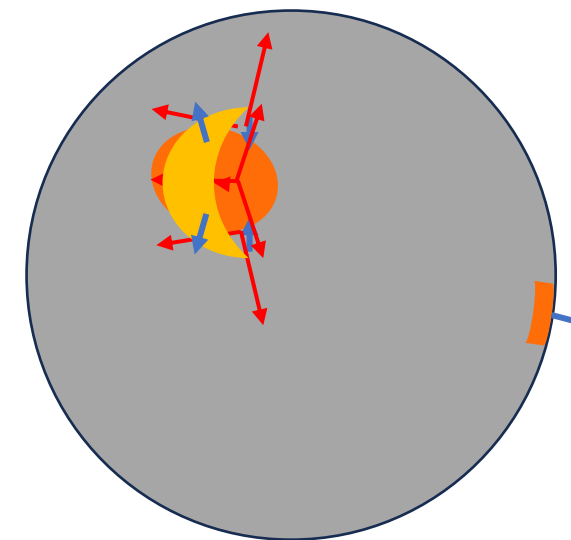


- Theoretical interpretation (in terms of the magnetic-loop model)

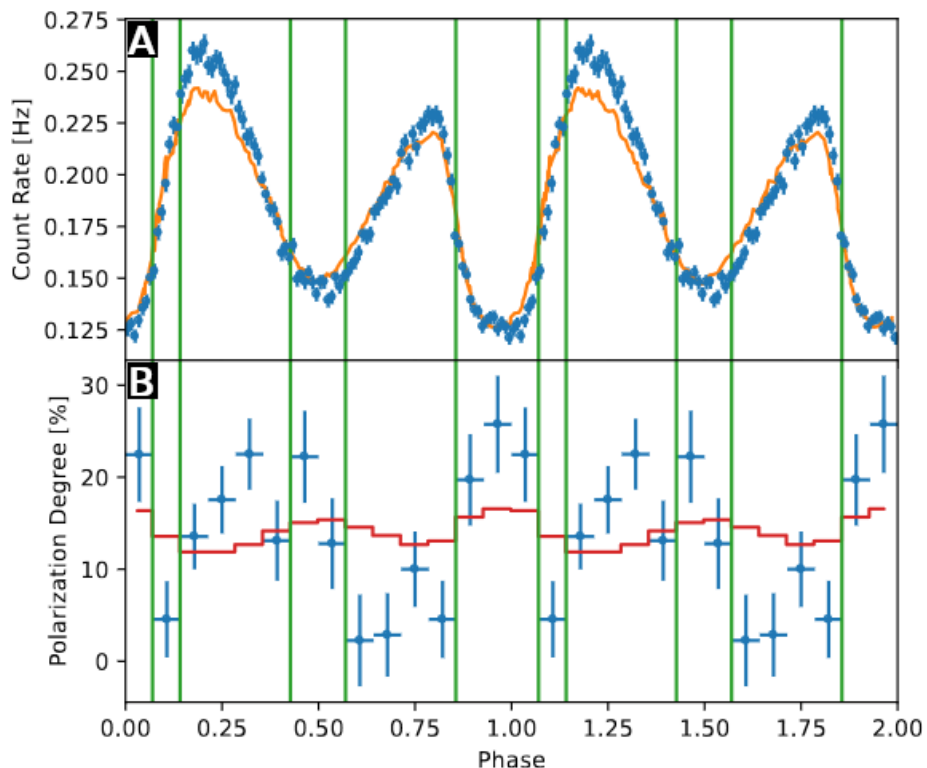


2 condensed-surface hotspots are present on the NS surface

The protons magnetic loop scatters away X-mode photons



- Theoretical interpretation (in terms of the magnetic-loop model)



2 condensed-surface hotspots are present on the NS surface

The protons magnetic loop scatters away X-mode photons

